Coordinated Beating of Algal Flagella is Mediated by Basal Coupling

Kirsty Y. Wan * **and Raymond E. Goldstein** *

*Department of Applied Mathematics and Theoretical Physics, University of Cambridge, Wilberforce Road, Cambridge CB3 0WA, UK

Submitted to Proceedings of the National Academy of Sciences of the United States of America

Cilia and flagella often exhibit synchronized behavior; this includes phase-locking, as seen in Chlamydomonas, and metachronal wave formation in the respiratory cilia of higher organisms. Since the observations by Gray and Rothschild of phase synchrony of nearby swimming spermatozoa, it has been a working hypothesis that synchrony arises from hydrodynamic interactions between beating filaments. Recent work on the dynamics of physically separated pairs of flagella isolated from the multicellular alga Volvox has shown that hydrodynamic coupling alone is sufficient to produce synchrony. However, the situation is more complex in unicellular organisms bearing few flagella. We show that flagella of Chlamydomonas mutants deficient in filamentary connections between basal bodies display markedly different synchronization from the wildtype. We perform micromanipulation on configurations of flagella and conclude that a mechanism, internal to the cell, must provide an additional flagellar coupling. In naturally-occurring species with 4, 8 or even 16 flagella, we find diverse symmetries of basal-body positioning and of the flagellar apparatus that are coincident with specific gaits of flagellar actuation, suggesting that it is a competition between intracellular coupling and hydrodynamic interactions that ultimately determines the precise form of flagellar coordination in unicellular algae.

Chlorophyte | *Prasinophyte* | *eukaryotic algae* | *internal coupling* | *flagellar synchronization* | *basal fibers*

Significance Statement

In areas as diverse as developmental biology, physiology and biomimetics there is great interest in understanding the mechanisms by which active hair-like cellular appendages known as flagella or cilia are brought into coordinated motion. The prevailing theoretical hypothesis over many years is that fluid flows driven by beating flagella provide the coupling that leads to synchronization, but this is surprisingly inconsistent with certain experimentally observed phenomena. Here we demonstrate the insufficiency of hydrodynamic coupling in an evolutionarily significant range of unicellular algal species bearing multiple flagella, and suggest the key additional ingredient for precise coordination of flagellar beating is provided by contractile fibers of the basal apparatus.

Introduction

Possession of multiple cilia and flagella bestows significant evolutionary advantage upon living organisms only if these organelles can achieve coordination. This may be for purposes of swimming (1, 2), feeding (3), or fluid transport (4, 5). Multiciliation may have evolved first in single-celled microorganisms due to the propensity for hydrodynamic interactions to couple their motions, but was retained in higher organisms, occurring in such places as the murine brain (6) or human airway epithelia (7). Since Sir James Gray first noted that "automatic units" of flagella beat in "an orderly sequence" when placed side by side (8), others have observed the tendency for nearby sperm cells to undulate in unison or aggregate (9, 10), and subsequently the possible hydrodynamic origins of this phenomenon have been the subject of extensive theoretical analyses (2, 5, 11). Despite this, the exclusiveness and universality of hydrodynamic effects in the coordination of neighboring cilia and flagella remains unclear.

We begin by considering one context in which hydrodynamic interactions are sufficient for synchrony (12). The alga *Volvox carteri* (VC) is perhaps the smallest colonial organism to exhibit cellular division of labor (13). Adult spheroids possess two cell types: large germ cells interior of an extracellular matrix grow to form new colonies, while smaller somatic cells form a dense surface covering of flagella protruding into the medium, enabling swimming. These flagella generate waves of propulsion which despite lack of centralized or neuronal control ("coxless") are coherent over the span of the organism (14). In addition, somatic cells isolated from their embedding colonies (Fig. 1A) beat their flagella in synchrony when held sufficiently close to each other (12). Pairwise configurations of these flagella tend to synchronize in-phase (IP) when oriented with power strokes in the same direction, but antiphase (AP) when oriented in opposite directions, as predicted (15) if their mutual interaction were hydrodynamic. Yet, not all flagellar coordination observed in unicellular organisms can be explained thus. The lineage to which *Volvox* belongs includes the common ancestor of the alga *Chlamydomonas reinhardtii* (CR) (Fig. 1B), which swims with a familiar in-phase breaststroke with twin flagella that are developmentally positioned to beat in *opposite* directions (Fig. 1C,D). Yet, a *Chlamydomonas* mutant with dysfunctional phototaxis switches stochastically the actuation of its flagella between IP and AP modes (15, 16). These observations led us to conjecture (15) that a mechanism, internal to the cell, must function to overcome hydrodynamic effects.

Pairs of interacting flagella evoke no image more potent than Huygens' clocks (17): two oscillating pendula may tend towards synchrony (or anti-synchrony) if attached to a common support, whose flexibility providing the necessary coupling. Here we present a diverse body of evidence for existence of a biophysical equivalent to this mechanical coupling, which in CR and related algae we propose is provided ultrastructurally by prominent fibers connecting pairs of basal bodies (BB) (18) that are known to have contractile properties. Such filamentary connections are absent in configurations of two pipette-held uniflagellate cells and defective in a class of CR mutants known as *vfl* (Fig. 1B). We show in both cases that the synchronization states are markedly different from the wildtype breaststroke.

Seeking evidence for the generality of putative internal control of flagellar coupling in algal unicells, we use light microscopy, high-speed imaging and image-processing to elucidate the remarkable coordination strategies adopted by quadri-, octo-, and hexadecaflagellates, which possess networks of basal, interflagellar linkages that increase in complexity with flagella number. The flagellar apparatus, comprising BBs, connecting fibers, microtubular rootlets and the transition regions of axonemes, is among the most biochemically and morphologically complex structures occurring in eukaryotic flagel-

Reserved for Publication Footnotes

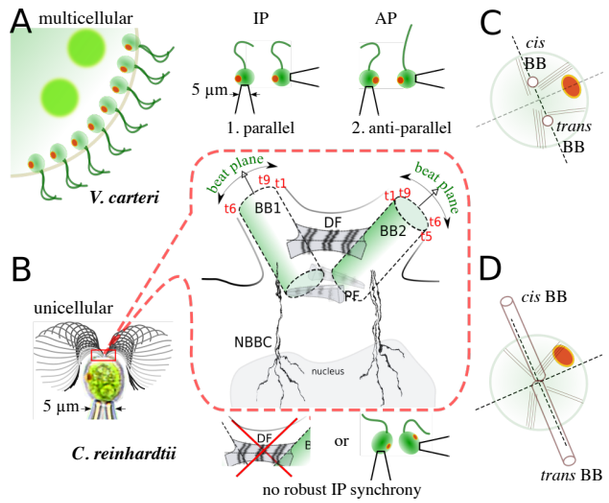

Fig. 1: Flagellar synchronization in multi- vs uni- cellular algae. A) Pairs of isolated, somatic flagella of *V. carteri* (VC) tend to synchronize either in in-phase (IP) or anti-phase (AP) depending on their relative orientation. B) *C. reinhardtii* (CR) flagella maintain position 2 yet swims a robust IP breaststroke that is lost i) by mutation of the distal fiber (DF), and ii) in pairs of nearby uniflagellate cells. C+D) Ultrastructure comprising basal bodies (BBs), rootlets, and eyespot in VC and CR. [PF - proximal fiber(s); NBBC - nuclear-basal-body connectors; t1 − 9: numbered microtubule triplets.]

lates (19). The significance of basal coupling relative to hydrodynamics is highlighted, especially in maintaining relative synchrony in diametrically-opposed pairs of flagella. Our study reconciles species-specific swimming gaits across distinct genera of green algae with the geometry of flagellar placement and symmetries of their differing basal architecture – so often a key phylogenetic character (20).

While many features of eukaryotic flagellar axonemes are conserved from algae to mammals (e.g. composition by microtubules, motive force generation by dyneins, signal transduction by radial-spokes/central pair (16)), far greater diversity exists in the coordination of multiple flagella. Such strategies are vital not only in microswimmers bearing few flagella, but also in ciliary arrays. In mice defects in structures known as basal feet can cause ciliopathies (21), while the striated (kinetodesmal) fibers in *Tetrahymena* help maintain BB orientation and resist hydrodynamic stresses (22). Insights from primitive flagellates may thus have significant broader implications.

Results

Synchronization of Chlamydomonas flagella. The basic configuration of two flagella appears in multiple lineages by convergent evolution, e.g. in the naked green alga *Spermatozopsis* (23), in gametes of the seaweed *Ulva* (24), and in swarm cells of *Myxomycetes* (25). CR exemplifies the isokont condition. Cells ovoid, $\sim 5\,\mu$m radius, have flagella $\sim 1.5\times$ body-length and distinguishable by BB age. During cell division each daughter retains one BB from the mother (26) which becomes associated with the *trans*-flagellum, while a second is assembled localizing near the eyespot and associates with the *cis*-flagellum (Fig. 1B,D). When both flagella prescribe identical beats a nearly-planar breaststroke results, which is highly recurrent and stable to perturbations (27). Yet despite extensive research (28–32) exactly how this IP breatstroke is achieved has remained elusive; coupling of the flagella pair may be by i) hydrodynamics, ii) drag-based feedback due to cell-body rocking, or iii) intracellular means.

CR cells turn by modulation of bilateral symmetry. During phototaxis (33) photons incident on the eyespot activate voltage-gated calcium channels which alter levels of intracellular calcium, leading to differential flagellar responses. Ionic fluctuations (e.g. Ca^{2+}) alter not only the flagellar beat, but also the synchrony of a pair. Gait changes involving transient loss of synchrony (called 'slips'), occur stochastically at rates sensitive to such environmental factors (15, 27, 34) as temperature, light, chemicals, hydrodynamics, and age of cell culture. In free-swimming cells, slips can alter the balance of hydrodynamic drag on the cell body, producing a rocking motion that promotes subsequent resynchrony of flagella (31), but this does not explain the robust IP synchrony in cells held immobilized on micropipettes (16, 29), nor the motility of isolated and reactivated flagellar apparatuses (35). The altered beat during slips is analogous to the freestyle gait (AP in Fig. 1) characterized in the phototaxis mutant *ptx1*, which stochastically transitions between IP and AP gaits (15, 16). The dependence of CR flagellar synchronization state on physiology through temperature or ionic content of the medium (27) leads us now to the possibility for intracellular coupling of flagella.

Early work (18) identified thick fibers connecting the two *Chlamydomonas* BBs, including a $300 \times 250 \times 75$ nm^3 bilaterally symmetric distal fiber (DF), bearing complex striation patterns with a periodicity of ~ 80 nm (Fig. 1B). Striation periodicity varies across species, and is changeable by chemical stimuli – indicating active contractility (36). The DF contains centrin, also found in NBBCs (Fig. 1B) which are involved in localization of BBs during cell division (37). The two BBs have an identical structure of 9 triplet microtubules which form a cartwheel arrangement (38). Importantly, the DF lies in the plane of flagellar beating, and furthermore attaches to each BB at the *same* site relative to the beating direction of the corresponding flagellum (Fig. 1B). This inherent rotational symmetry makes the DF uniquely suited to coordinating the in-phase *Chlamydomonas* breaststroke.

Hypothesizing a key role for the DF in CR flagellar synchrony we assess the motility of the mutant *vfl3* (CC1686, *Chlamydomonas* Center), with DFs missing, misaligned or incomplete in a large fraction of cells (36). Swimming is impaired – many cells rotate in place at the chamber bottom. In *vfl3* the number of flagella $(0-5)$, their orientation and localization on the cell body, as well as cell size are abnormal. BBs still occur in pairs, but not every BB will nucleate a flagellum (39), thus allowing flagella number to be odd. However no structural or behavioral defects were observed in the flagella (36).

A number of representative configurations of flagella occur in *vfl3*, for cells bearing 2 or 3 flagella (Fig. 2A-F). Fig. 2G presents the wild-type case. We consider pairwise interactions between flagella. For each flagellum, we extract a phase $\phi(t)$ from the high-speed imaging data by interpolating peaks in the standard deviation of pixel intensities measured across pre-defined regions of interest. *vfl3* flagellar beating frequencies are found to be more variable than the wildtype, so we elect to determine phase synchrony between pairs of flagella via a stroboscopic approach. Given phases ϕ_1, ϕ_2 we wish to characterize the distribution $\mathcal{P}_C(\chi)$ of $\chi = \phi_2 \bmod 2\pi|_{t:\phi_1 \bmod 2\pi = C}$. Thus, the phase of flagellum 2 is measured *conditional* on the phase of flagellum 1 attaining the value C. From long timeseries we determine χ by binning $[0, 2\pi]$ into 25 equi-phase intervals centered around $\{C_k, k = 1, \cdots, 25\}$ to obtain the N_k corresponding time points for which $\phi_1 \bmod 2\pi$ falls into the kth interval. The distribution of this conditional phase $\chi^k := \{\phi_2(t_i), i = 1, \cdots, N_k\}$, which is peaked when oscillators phase-lock and uniform when unsynchronized, can then be displayed on a circular plot by conversion to a colormap. In Fig. 2, we take $k = 1$. Phase vectors can be summed and averaged to define a synchronization index

$$\mathcal{S} = \frac{1}{25}\sum_{k}^{25}\left|\frac{1}{N_k}\sum_{j}^{N_k}\exp(i\chi_j^k)\right|, \qquad [1]$$

where $\mathcal{S}_k = 1$ (perfect synchrony) and $\mathcal{S}_k = 0$ (no synchronization).

In *vfl3*, steric interactions between nearby flagella (e.g. Fig. 2A) can lead to intermittent beating and reduction in beat frequency. Even when measured beat frequencies differ for flagella on the same cell, periods of phase-locking are observed, which we attribute to hydro-

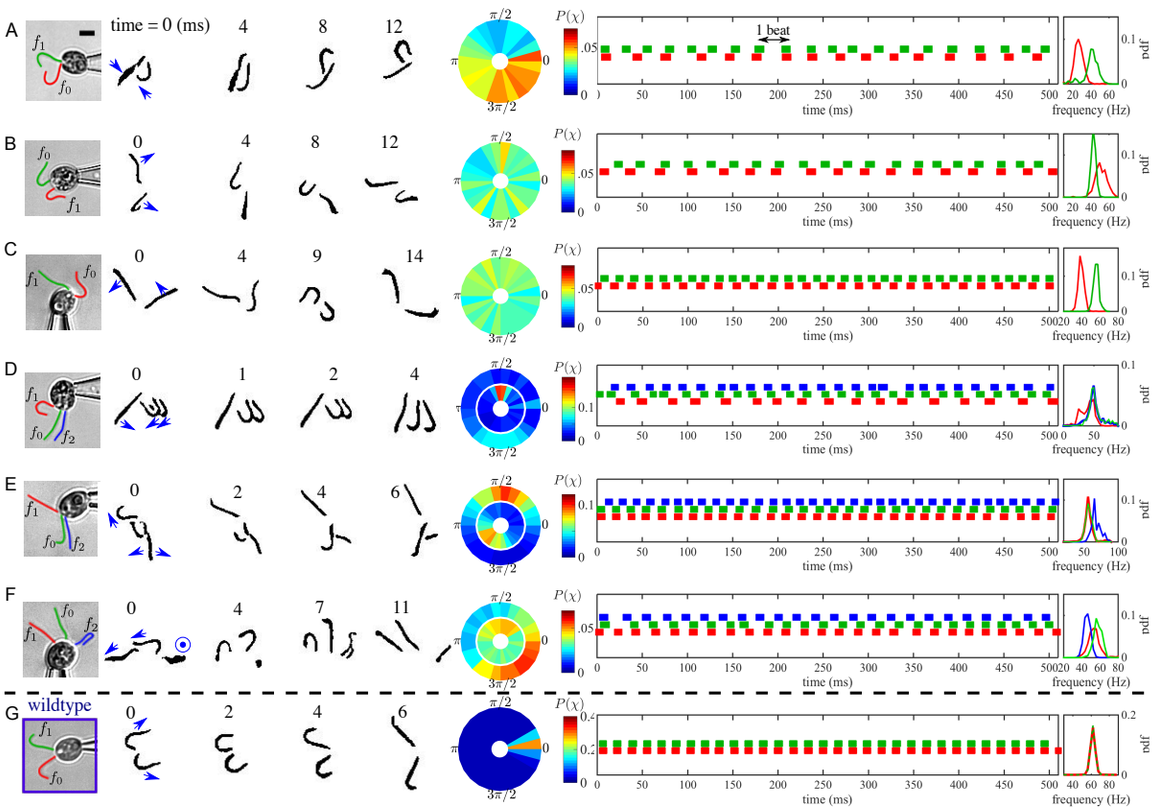

Fig. 2: The CR mutant *vfl3* has defective DF, abnormal flagella number and orientation. Scale bar: 5 μm. Shown are groups of 2 or 3 flagella in orientations of interest. (A,B) are toward or away-facing and flagella-like i.e. anti-parallel; (C) is cilia-like i.e. parallel; (D,E) exhibits clear hydrodynamic phase-locking of closely-separated parallel or anti-parallel pairs of flagella. Only (F) has a non-planar aspect: flagellum f_2 points out of the page. Power stroke directions are indicated by the arrows. Phase distributions $\mathcal{P}_0(\chi)$ of flagellum $f_{1,(2)}$ conditional on the phase of flagellum f_0 are shown on circular plots (in D-F: f_1 for the inner ring and f_2 for the outer). For A-C, $S_{1,0} = 0.20, 0.04, 0.04$, and for D-F, $(S_{1,0}, S_{2,0}) = (0.30, 0.49), (0.53, 0.40), (0.02, 0.01)$. In contrast for the wildtype, $S_{1,0} = 0.96$ (panel G). Discretized phases are plotted as "footprints" with length proportional to beat-cycle duration, with pdfs of beat frequencies.

dynamic interactions (12, 15, 40) (see also SI Video 1). In the triflagellates of Figs. 2D&E, beating of a given flagella pair becomes strongly coupled, with IP or respectively AP synchrony being preferred when flagella are oriented with power strokes parallel or respectively anti-parallel (compare f_0,f_2 in D with f_0,f_2 in E). Even biflagellate *vfl3* cells with a native CR-like configuration cannot perform IP breaststrokes (e.g. Fig 2B). In contrast wildtype CR flagella operating over a large frequency range are able achieve robust synchrony, despite intrinsic *cis*/*trans* frequency differences of up to 30% during slips, or conditions of physiological stress such as deflagellation (16). Thus possession of functional or complete DFs appears necessary for CR flagellar synchrony.

Micromanipulation of flagellate algae. Next we ask whether the CR breaststroke can instead be produced by hydrodynamic interactions. Use of flagella belonging to *different* cells offers a tractable alternative to removal by mutation of such physical connectors as the DF. We construct, by micromanipulation, configurations of two flagella that cannot be coupled other than through the immersing fluid.

In Fig. 3A, one flagellum was removed from each of two wildtype CR cells by careful mechanical shearing (Materials and Methods), so that a CR-like arrangement comprising one *cis* and one *trans* flagellum is assembled. Despite similarity with the wildtype configuration, no sustained IP breaststrokes were obtained. Closely separated (<5 μm) pairs exhibit periods of phase locking. Beat frequencies of these flagella are found to be more noisy than their counterparts in intact CR cells, and consequently measured phase-locking is not robust ($S = 0.08$). The conditional (stroboscopic) phase χ (Fig. 3A) is peaked weakly about π indicating a tendency for AP synchronization, but the IP state is also possible. This bistability is not species-specific; we rendered uniflagellate [see also (12)] pairs of pipette-held VC somatic cells (normally biflagellate) and placed them in a similar configuration (Fig. 3B). Analysis of the resulting pairwise flagellar interactions indicates a strong preference for AP synchronization, though the IP is again observed (see SI Videos 2 & 3). Accordingly, the phase stroboscope is now strongly peaked near $\chi = \pi$ (with $S = 0.67$).

The existence, stability, and frequency of IP and AP states are wholly consistent with a basic theory (40) which models a pair of hydrodynamically coupled flagella as beads rotating on springs with compliant radii R separated by distance ℓ (see SI Text). Assuming $R \ll \ell$, either IP or AP states of synchrony are predicted to be stable depending on whether the beads are co- or respectively counter-rotating (15, 40). Thus, CR-like configurations should tend to AP synchrony. However in our experiments, flagella often come into such close proximity during certain phases of their beat cycles that the far-field assumptions of the original model breakdown. Non-local hydrodynamic interactions between different portions of flagella must now be considered for the true flagellar geometry (rather than in a phase-reduced bead model). In particular undulating filaments can be driven by fluid-structure interactions into either IP or AP oscillating modes depending on initial relative phase (41). The inherent stochasticity of flagellar beating (27) thus leads to transitions between IP and AP states (Fig. 3). Hydrodynamic effects are notably stronger in the case of VC than CR, due to reduced screening by a smaller

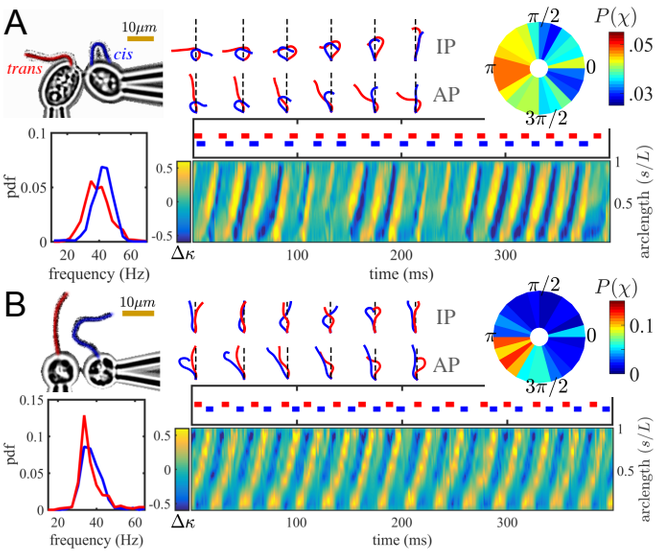

Fig. 3: Coupling A) two CR flagella (one *cis*, one *trans*) and B) two uniflagellated VC somatic cells, both in anti-parallel configuration. In both cases IP and AP states are observed, the AP being preferred. In B), hydrodynamic coupling is notably stronger. The pairwise curvature difference $\Delta\kappa$ (μm^{-1}) plotted on the same time axis as phase "footprints", shows propagating high-curvature bends which are coincident during IP, or alternating during AP.

cell body and a distinctive upward tilt of the flagellar beat envelope. During evolution to multicellularity, this latter adjustment of BB orientation (Figs. 1C&D) facilitates beating of flagella confined within a spherical colony. The CR mutant *ptx1* also displays noisy transitions between IP and AP gaits (15) due to an unknown mutation, the implications of this we shall return to later (see Discussion).

The similarity of two flagellar waveforms in any given state (IP or AP) can be compared. For ease of visualization, waveforms discretized at equidistant points are ordered from base to tip: $\mathbf{f}_i^{\mathrm{L}}$, $\mathbf{f}_i^{\mathrm{R}}$ for $i = 1, \cdots N_p$, and rescaled to uniform total length. These are rotated by $\mathcal{T}(\alpha)$ through angle α between the horizontal and line of offset between the BBs. We denote by $\mathbf{f}^{\mathrm{L}} \rightarrow \mathbf{f}'^{\mathrm{L}} = \mathcal{T}(\mathbf{f}^{\mathrm{L}} - \mathbf{m})$ and $\mathbf{f}^{\mathrm{R}} \rightarrow \mathbf{f}'^{\mathrm{R}} = \mathcal{T}(\mathbf{f}^{\mathrm{R}} - \mathbf{m})$, with $\mathbf{m} = (\mathbf{f}_1^{\mathrm{L}} + \mathbf{f}_1^{\mathrm{R}})/2$, and compare the resulting shape symmetries during IP and AP states (Figs. 3A&B, stacked). The synchronization index of Eq. 1, while suitable for identifying presence or absence of phase synchrony, does not discriminate between AP or IP states. Instead, we compute the pairwise curvature difference $\Delta\kappa(t,s) = \kappa_L - \kappa_R$ as a function of time (t) and normalized arclength (s), where κ_L, κ_R are *signed* curvatures for the left and right flagellum according to their respective power stroke directions. During IP and AP synchrony, $\Delta\kappa$ exhibits a wave pattern at the common or phase-locked frequency. Principal or high-curvature bends propagate from flagellum base to tip in accordance with the mechanism of flagellar beating in these species (0.897 ± 0.213 mm/s for CR, and 0.914 ± 0.207 mm/s for VC). In summary, we have established in two species that robust IP synchrony akin to the CR-breaststroke does not arise from hydrodynamic coupling between two co-planarly beating flagella arranged in a CR-like configuration, even when beat frequencies are comparable.

Moreover the propensity for algal flagella to be deformable by hydrodynamic loading (12) – e.g. flows generated by nearby flagella, suggests an internal coupling must be present to compensate in such cases where fluid interactions are contrary to the desired mode of propulsion by flagella in the organism. Given this delicate interplay, will a dramatic perturbation to the state of hydrodynamic interactions between flagella affect their *native* mode of coordination? For this we require an organism with more than two flagella. *Tetraselmis* is a thecate quadriflagellate, and amenable to micromanipulation. Fig. 5A depicts a pipette-immobilized *Tetraselmis* cell with flagella free to beat in a pattern qualitatively similar to free-swimming cells observed under identical conditions (see SI Video 4), in which flagella maintain a transverse gallop (next section, and Fig. 4D). One flagellum was then trapped inside a second pipette with suction so as to completely stall its beating, with minimal disruption to the cell. Flagellar dynamics were monitored and interflagellar correlation functions computed (Fig. 4B), showing that the prior beat patterns continue (Fig. 4C). The small increase in beat frequency in the remaining flagella ($\sim 5\%$) is consistent with calcium-induced frequency elevation by mechanosensation. This remarkable ability for the cell to sustain its coordination pattern strongly implicates internal beat modulation.

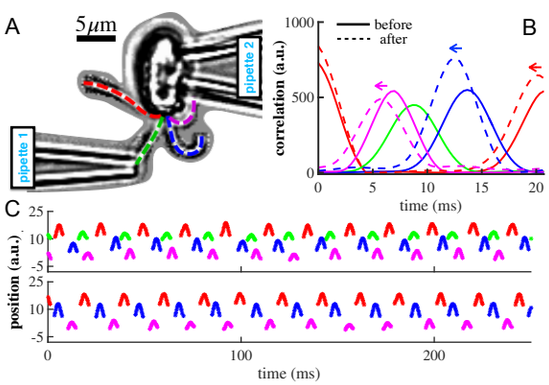

Fig. 4: A) Stalling the flagellum beat in *Tetraselmis suecica*. B) Beat correlations for each flagellum relative to a reference flagellum (red) computed before and after manipulation, shows period shift but no change in the order of flagella actuation. C) Timeseries or "footprints" delineate positions of flagella (labelled as in A) before (above) and after (below) manipulation.

Symmetries of the algal flagellar apparatus. Such a hypothesis brings us now to further detailed study of a large number of lesser-known species that have differing or more complex basal architectures and which in turn, we find to display varied and novel flagellar coordination strategies. While it is believed that Volvocine green algae (including VC) derived from *Chlamydomonas*-like ancestors, the general classification of Viridiplanta (green plants) has undergone repeated revisions due to the enormous variability that exists in the form and structure exhibited by its member species. Features, both developmental (mitosis, cytokinesis) and morphological (number, structure, arrangement of flagella, nature of body coverings such as scales and theca), have served as key diagnostics for mapping the likely phylogenetic relationships existing between species (42, 43).

We selected unicellular species of evolutionary interest to exemplify configurations of $2, 4, 8$ or even 16 flagella (SI Videos 6, 7&8). These include (Fig. 5) distinct genera of bi- and quadri- flagellates – both occurring abundantly in nature, the rare octoflagellate marine Prasinophyte known as *Pyramimonas octopus*, and its relative *Pyramimonas cyrtoptera* – the only species known with 16 flagella (44). Indeed only three *Pyramimonas* species have 8 flagella during all or parts of its cell cycle (45–47). Several species belong to the Prasinophytes – a polyphyletic class united through lack of similarity with either of the main clades (Chlorophyta and Streptophyta), whose > 16 genera and > 160 species (48) display a remarkable variability in flagella number and arrangement that is ideal for the present study.

Distinct quadriflagellate gaits were identified, involving particular phase relations between flagella. An analogy may be drawn with quadruped locomotion (Fig. 5&6). For measured flagellar phases ψ_j (flagellum index j) we compute the matrix $\Delta_{ij} = \psi_i - \psi_j \quad (i, j = 1, \ldots, 4)$, where $\Delta_{ij} = \Delta_{ji}$, $\Delta_{ii} = 0$, and $\Delta_{ik} = \Delta_{ij} + \Delta_{jk}$.

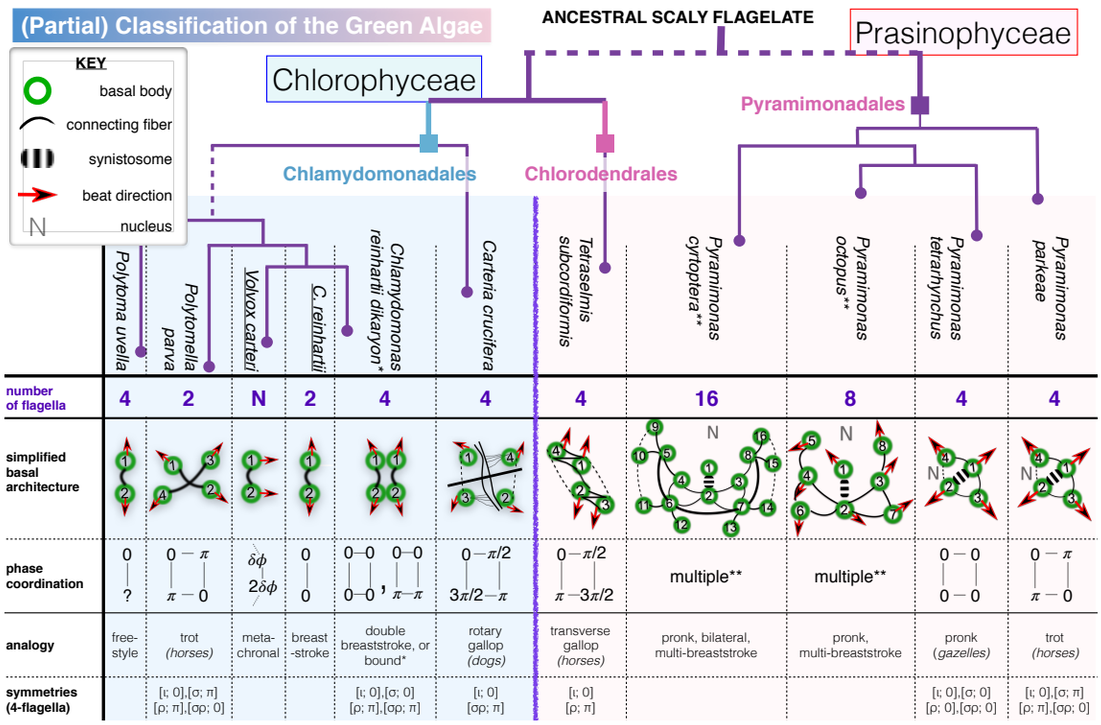

Fig. 5: Algal species are compared in terms of phylogeny, number and orientation of flagella, arrangement of BBs/basal architecture (see also SI Text), and patterns of coordination defined by the relative phases between flagella. Vertical lines approximate the relative phylogenetic distance from a putative flagellate ancestor (SI Text) (only partial branchings are shown). Free-swimming quadriflagellate gaits are readily identified with quadruped locomotion, revealing the symmetries of an underlying oscillator network. [* Quadriflagellate dikaryons of CR gametes perform a double breaststroke gait with the same symmetries as the 'pronk' (SI Video 5), but this gives way to a 'bound' gait when both sets of flagella undergo phase slips simultaneously. ** See SI Videos 7&8.]

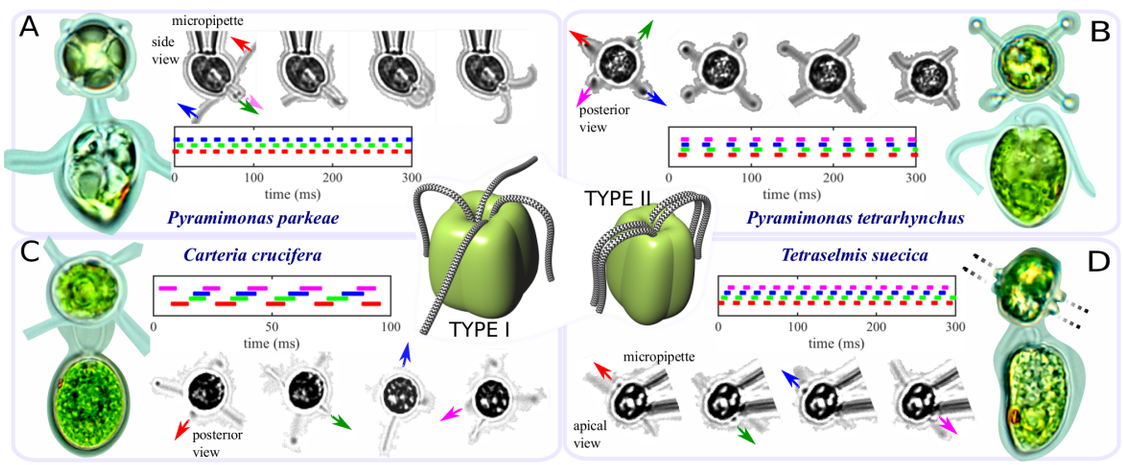

Fig. 6: In free-living quadriflagellates, flagella can be arranged in one of two possible configurations (types I,II) – type II is unusual. Gaits of coordination are diverse and species-specific, including the trot (A), pronk (B), rotary (C) and transverse (D) gallops. Representative species imaged from top and side, show locations of eyespots and chloroplast structures. Timeseries of phases are measured for pipette-held cells in A,D, and free-swimming cells in B,C.

Each gait is then associated with a 3-tuple of phase differences: $[\Delta_{12}\,\Delta_{13}\,\Delta_{14}]$. For instance, *P. parkeae* swims with two pairs of precisely alternating breaststrokes akin to the 'trot' of a horse (Fig. 6A, SI Video 6), its 4 isokont flagella insert anteriorly into an apical pit, emerging in a cruciate arrangement typical of quadriflagellates (Fig. 6, type I). The phase relation $[\Delta_{12}\,\Delta_{13}\,\Delta_{14}] = [\pi\,0\,\pi]$ is seen in both free-swimming and micropipette-held cells. A Chlorophyte alga *Polytomella* sp. *parva* (Fig. 5), was also found to display this gait.

Two further gaits (SI Video 6) occur in the type *Pyramimonas* species *P. tetrarhynchus* (49), a freshwater alga. The first we term the 'pronk', where all flagella synchronize with zero phase difference (Fig. 6B). In the second, flagella beat in a sequence typical of the transverse gallop in quadrupeds (Fig. 5). *P. tetrarhynchus* swims preferentially with the latter gait, while pronking can occur when the cell navigates near walls/obstacles, or when changing direction. The rotary gallop, with flagella beating CCW in orderly sequence (Fig. 6C, SI Video 6) occurs in the Volvocale *Carteria crucifera*. Finally in *Tetraselmis*

(recall Fig. 4) the flagella separate distally into pairs (Fig. 6, type II). Cells display the transverse gallop when free-swimming or pipette-held despite strong hydrodynamic interactions within each pair. An alternate synchronous gait of four flagella has been reported in this species (50), but was not observed under our experimental conditions.

Ordinarily, motive gaits whereby the limbs of a quadruped or arthropod are actuated in precise patterns are produced by networks of coupled oscillators controlled by a central pattern generator (CPG) or equivalent (51, 52). Analogously, can we relate symmetries of the flagellar apparatus to gait symmetries, with contractile filaments providing the putative coupling? We focus on quadriflagellates, where an abundance of species makes possible comparative study (Fig. 6). Spatial symmetries of flagella $\mathbf{X}_j$ (indexed by $j = 1, 2, 3, 4$) are represented as permutations σ of $\{1, 2, 3, 4\}$, so that $\mathbf{X}_k(t) = \mathbf{X}_{\sigma(k)}(t)$ for all times t. Periodic gaits also possess temporal symmetries: if T is the gait period, then for the kth oscillator $\mathbf{X}_k(t) = \mathbf{X}_k(t + T)$ for all t. We normalize T to 2π and consider invariance of flagella under phase shifts ϕ taken modulo $T/2\pi$; the pair $[\sigma, \phi]$ denotes a spatial-temporal symmetry of the $\{\mathbf{X}_j\}$, where

$$\mathbf{X}_k(t) = \mathbf{X}_{\sigma(k)}(t - \phi). \qquad [2]$$

and $k = 1, \cdots, 4$. The set of spatiotemporal symmetries may admit a (symmetry) group under composition:

$$[\sigma_1; \phi_1] \circ [\sigma_2; \phi_2] = [\sigma_1\sigma_2; \phi_1 + \phi_2], \qquad [3]$$

to be matched with known quadruped/quadriflagellate gaits. For a basal morphology of a rectangularly symmetric network (51) with distinct lengthwise and crosswise couplings – in Fig. 5 (phase coordination) represented by lines of differing lengths, spatial symmetries include ι (the identity, fix everything), $\sigma = (12)(34)$ (reflect in y-axis), $\rho = (13)(24)$ (reflect in x-axis), and $\sigma\rho = (14)(23)$ (interchange of diagonals). In Fig. 5, we attach named gaits and associated symmetry groups to the species in which they are observed. Additionally some quadriflagellates display a 'stand' gait (a transient rest phase where no flagellum beats); this has the largest number of symmetries: $[\iota; \phi]$, $[\sigma; \phi]$, $[\rho; \phi]$, $[\sigma\rho; \phi]$, for arbitrary ϕ.

Can such a network resemble coupling of algal flagella? Despite significant variation across species, linkages or roots connecting BBs are key systematic characters. These can be microtubular or fibrillar. Microtubular roots, which were probably asymmetric in very early flagellates (20), position BBs and attached flagella during development (two per BB: termed left, right). The right root is generally 2-stranded, and together with the left-root (X-stranded) form an X-2-X-2 cruciate system characteristic of advanced green algae [$X = 4$ in CR (18)]. Only one absolute configuration of BBs exists for each species and its mirror-symmetric form is not possible (53). For instance in CR two BBs emerge at $70 - 90^\circ$ with a clockwise (CW) offset characteristic of advanced biflagellate algae (Fig. 1D), in contrast many evolutionarily more primitive flagellates have BBs oriented with a counter-clockwise (CCW) offset (20). Fibrillar roots, classified as system I or II (43) become more numerous with flagella number. These are generally contractile, likely contributing to interflagellar coupling. Each BB is unique up to the imbrication of its member tubules – a constant positional relationship pertains between its two roots and a principal connecting fiber linking the two ontogenetically oldest BBs, labelled 1,2 in keeping with convention (53, 54). It is this fiber that is mutated in *vfl*3 mutants (recall Fig. 2).

Take a quadriflagellate species for which the basal architecture is known, and consider its associated swimming mode. In *P. parkeae* (Fig. 6A), a prominent (striated) distal fiber called the synistosome links BBs $1, 2$ only (55), so that the coupling is different between different pairs. In the advanced heterotroph *Polytomella parva* which swims with a comparable gait, flagella form opposing V-shaped pairs with different coupling between pairs (56). In *Tetraselmis*, the flagella separate distally into two nearly collinear pairs with BBs forming a single zig-zag array (Fig. 5), in a state thought to have arisen from rotation of two of the flagellar roots in an ancestral quadriflagellate. Transfibers which are functionally related to the *Chlamydomonad* PF and DF, connect alternate BBs, while BBs within the same pair are linked by Z-shaped struts (57), emphasizing a diagonal connectivity which may explain its transverse gallop (Fig. 6D). In contrast the rotary gallop, prominent in *C. crucifera* (Fig. 6C) is more consistent with a square symmetric network involving near identical connectivity between neighboring flagella, than a rectangular one. Indeed the flagellar apparatus in this species has been shown to exhibit unusual rotational symmetry: BBs insert into an anterior papilla at the corners of a square in a cruciate pattern (class II *sensu* Lembi (58)) and are tilted unidirectionally in contrast to the conventional V-shapes found in *Chlamydomonas* and *Polytomella*. (Here DFs rather than link directly to BBs, attach to rigid electron-dense rods extending between them (58).) Finally, a different network of couplings appears when two biflagellate CR gametes fuse during sexual reproduction (59) to form a transiently quadriflagellate dikaryon (similar to configuration II, Fig. 6). Here, original DFs between *cis* and *trans* remain but new fibers do not form between pairs of flagella of unlike mating type. Strong hydrodynamic coupling due to their physical proximity results in a striking *double* bilateral breaststroke (SI Video 5). A 'bound'-like gait can appear if both sets of CR flagella slip together (Fig. 5).

Thus, algal motility appears to be constrained by the form of underlying coupling provided by a species-specific configuration of BBs and connecting fibers. The case of octo- and hexadeca- flagellates swimming is more complex (SI Video 7,8), limited by the number of species available for study, and presence of a large number of fibrous structures whose identities remain unknown. A consistent numbering system for BBs has greatly facilitated the study of flagellar transformation in algae with many flagella, which we adopt (53, 54). As in other *Pyramimonas* BBs $1, 2$ remain connected by a large synistosome (Fig. 5). In *P. octopus* up to 60 individual fibers establish specific connections with specific BB triplets, in addition to 6-8 rhizoplasts linking the basal apparatus to the nucleus. Numerous rhizoplasts and connecting fibers also exists in *P. cyrtoptera* but were never resolved fully because of the untimely death of T. Hori (60). In *P. octopus* (Fig. 7) BBs arrange in a diamond (partially open to allow nuclear migration during mitosis). BB duplication is semi-conservative (61): 8 new BBs form peripheral to the existing ones during cell divi-

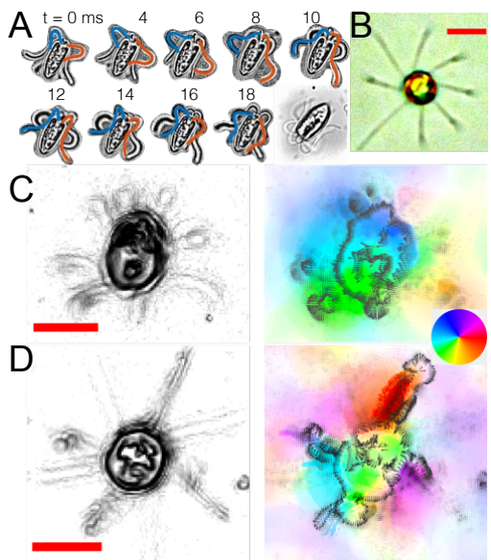

Fig. 7: *P. octopus* cell A) swims using multiple pairs of breaststrokes: highlighted are waveforms of one synchronous pair. In B), cell is at rest in a 'stand' gait in which no flagellum is active. C-D) Gradient images (left) identify the active subset of flagella (all, or 4 of 8), optical flow fields (right) show decay of beating-induced flow disturbance. Scale bars: 10 μm.

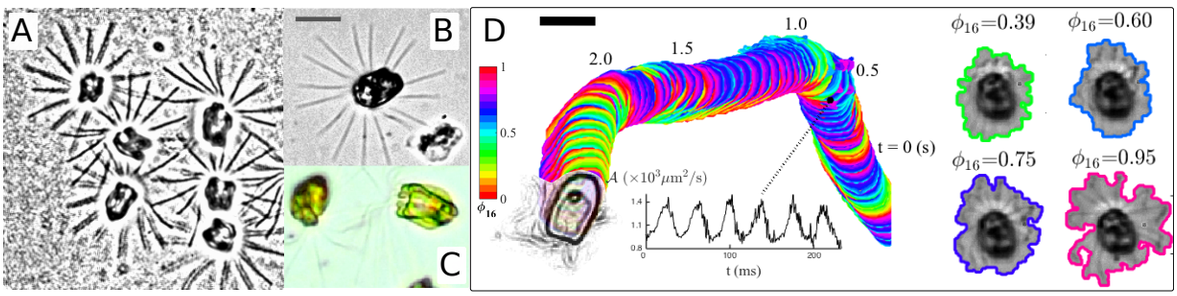

Fig. 8: In the rare Arctic species *P. cyrtoptera* flagella can remain at rest for seconds in a 'stand' gait (A-B). Cells appear yellow-green and lobed (C). (D) Pronking involving all 16 flagella (SI Video 8) is a common swimming gait. The cell body is tracked along a typical trajectory and colored by normalized phase ϕ_{16} (colorbar), computed from the area $\mathcal{A}(t)$ bounding the flagella which expands and contracts according to the periodicity of flagellar beating (shown here at 4 representative phases). Inset: time series of $\mathcal{A}$ over 6 successive cycles. Scale bars: 20 μm.

sion (54). The innermost BBs $(1, 2)$ assume the new position 1 in the two daughters (i.e. full maturation) after round 1 of cell division, but BBs $3, 4$ and 5-8 only reach maturation respectively after rounds $2, 3$ (47, 54). All 2^n BBs in a given cell reaches and thereafter remains at position 1 by the nth generation (cf *P. cyrtoptera* (44)).

In electron micrographs of *P. octopus*, flagellar beating is oriented in CCW sequence (47, 54) consistent with observed CW body rotation (viewed from above). Cells ≈ 20 μm in length, with yet longer flagella whose distal portions fold and recurve by the cell, swim at $200 \sim 300$ μm/s along helical paths. Diametrically opposite groups (usually but not exclusively pairs) of flagella beat synchronously with ordered phase shifts between groups (Fig. 7A, SI Video 7). In-phase coupling appears more robust in distinguished pairs (SI Video 7) reflecting prominent symmetries of the basal architecture: e.g. a large synistosome links BBs $1, 2$ whose flagella beat in opposite directions (Fig. 5). Compatible with its benthic nature, *P. octopus* display the 'stand' gait introduced previously (Fig. 7B) . Swimming motion resumes spontaneously when all 8 flagella reactivate (pronking), and the normal gait is reestablished within only 2 or 3 beats. A transient state in which beating occurs in 4 of 8 flagella (staggered) is observed Fig. 7D: in which actively beating flagella are identified by summing successive gradient images (in contrast ih Fig. 7C all 8 flagella are in motion). We visualise the flow disturbance imparted by flagellar beating using optical flow to monitor the migration of image pixels between frames, and estimate flow directions and magnitudes (62) (also Computer Vision toolbox, MATLAB, The MathWorks Inc.). Components of the $2D$ flow field were determined by minimizing an objective function subject to certain global (smoothness) or local (fidelity) constraints, and pixels delineating the same object are likely to have constant intensity. Unlike conventional PIV methods, this removes the need to seed the medium with foreign particles or tracers, and fluid flow due to motion can be obtained directly from optical data. Flow strengths decay rapidly away from boundaries of flagella as well as the cell body which is also in motion (Figs. 7C&D, right). More generally, gait transitions in these primitive algae can be dramatic and involve unusual flagellar coordination in response to external stimuli, and shall be explored further in a separate manuscript. Here, we reserve special attention to the *P. cyrtoptera* pronking gait, which displays striking hydrodynamic interactions.

Hydrodynamic synchronization in a hexadecaflagellate. *P. cyrtoptera* is the only hexadecaflagellate known (63). It is an Arctic species thought to have evolved when *P. octopus* failed to divide after duplication of chloroplasts and flagella. Measuring up to 40 μm, this is the largest *Pyramimonas* ever recorded. Its 16 flagella (32 when dividing), which are longer than the cell and emerge radially from a deep anterior flagellar pit (Figs. 8A&B), are used by the organism to attach to icy surfaces. The name *P. cyrtoptera* is derived from the Greek for *cyrtos* meaning "curved" and *pteron* meaning "wing", in reference to cell morphology. Light microscopy reveals a lobed structure with two pairs of split eyespots and the presence of two chloroplasts (Fig. 8C). *P. cyrtoptera* cells are stenothermal and euryhaline: growth becomes limited above 7-8°C. Once removed from their natural habitat where temperature variations are typically <2°C, cell cultures often prove fragile and difficult to maintain in the lab.

Hexadecaflagellate swimming presents an intriguing circumstance in which the distance of separation between flagella is so small that hydrodynamic coupling is inevitable. When fully splayed (Fig. 8B) the 16 flagella are separated on average by $360/16 = 22.5^\circ$ or 7.85 μm measured at a radial distance of 20 μm from the cell, compared to $360/8 = 45^\circ$ and twice this distance in *P. octopus*. In *P. cyrtoptera* the interflagellar distance is thus far below the critical length to achieve synchronization by hydrodynamics (12). Strong hydrodynamic interactions are evident between some or even all flagella (SI Video 8), none more so than during the pronk. Instead of tracking individual flagella (which beat in synchrony), we use the area $\mathcal{A}(t)$ bounding the flagella as proxy for phase of beat cycle (normalized):

$$\phi_{16}(t) = \left(\frac{t - t_n}{t_{n+1} - t_n}\right) \qquad [t_n \leq t \leq t_{n+1}], \qquad \textbf{[4]}$$

where t_n are discrete marker events corresponding to local maxima of $\mathcal{A}(t)$. Pronking occurs at a ~ 25 Hz (Fig. 8D). Significant hydrodynamic effects are also evidenced in cells swimming against surfaces, where flagella exhibit symplectic metachronal waves (SI Text).

Discussion

Insufficiency of hydrodynamics. The phenomenon of cooperative or synchronous beating of cilia and flagella has received growing attention, with hydrodynamic interactions historically assumed to be the major source of coupling. It is only recently (15, 31, 32) that researchers have begun to question this long-standing belief. Our approach was motivated in part by the freestyle gait (AP) in the CR phototaxis mutant *ptx1*, realizing that the wildtype IP breaststroke cannot be reconciled with hydrodynamic theory (15, 16). An additional ingredient, internal to the cell, must be maintaining IP synchrony in CR. The finding that entrainment of CR flagella by periodic external flows only occurs at frequencies close to the natural beat frequency and strengths greatly in excess of physiological values led Quaranta *et al* to a similar conclusion (32). The DF likely couples CR flagella, providing a degree of freedom that can reorient a flagellum at the BB through its contraction. In isolated and reactivated flagella apparatuses for example, the DF constricts in response to elevated extracellular calcium to reduce the opening angle between the two BBs (35). Since BBs nucleate/anchor flagella *and* function as centrioles during cell division, the DF can also be affected by mutations in BB duplication and segregation (36). This brings us back to the unusual flagellar coordination in *ptx1*, which is thought to possess two *trans*-like flagella (64). If BB signalling or connectivity is disrupted or weakened

in *ptx1*, stochastic IP/AP transitions can result when hydrodynamic interactions compete with a reduced intracellular coupling (15). Indeed, for all their DF defects, flagella of *vfl3* do not synchronize or only hydrodynamically when very close together (Fig. 2). Future work should seek to examine flagellar apparatuses of *ptx1* under electron microscopy. The failure of hydrodynamics to synchronize two flagella in a CR-like configuration, let alone two functionally distinct flagella such as a *cis* and a *trans* (16, 65), was shown by micromanipulation of two pipette-held cells (Fig. 2).

The diversity of coordination gaits in flagellate species (Fig. 5) implicates internal coupling as a generic remedy for this insufficiency of hydrodynamics. Indeed, non-uniqueness of stable quadriflagellate gaits for even identical configurations of 4 flagella is incompatible with existence of a single hydrodynamic mode. In some species a number of gait bifurcations can occur during free-swimming, involving modification or even cessation of beating in one or more flagella suggesting coordination is an active process. The significant perturbation to the hydrodynamic landscape resulting from immobilizing one flagellum in *T. suecica* was found to have little effect on the native coordination of the remainder (Fig. 4). Thus symmetries of flagellar gaits are much more species- than drag- dependent.

Intracellular coupling of flagella by contractile fibers. Gaits are defined by the relative phase between oscillators, which in the analogy of multi-legged locomotion, may be produced by CPG or pacemaker signals which in algae we conjecture to be mediated by the basal architecture. Flagellar apparatuses imaged by electron microscopy reveal species-specific networks of connections which increase in complexity with flagella number (19). Symmetries of an underlying network of structural couplings (51) likely translate downstream into symmetries of observed multiflagellate gaits (Fig. 5). The BB from which the flagellum nucleates is a center for conduction of morphogenetic and sensory information between flagella and other intracellular organelles. Although BBs are not essential for flagellar function (isolated axonemes continue to beat when reactivated in ATP (66, 67)), the contractility of inter-BB connections may contribute to coordination (68). In CR robust NBBCs descending near the DF link BBs to the nucleus (Fig. 1B) remain intact even after detergent lysis treatment (37), and can be induced by calcium to undergo significant contraction (69). Similarly rhizoplasts of scaly algae including *Pyramimonas* and *Tetraselmis* can contract and relax cyclically (43, 50). These species display frequent directional changes (mechanoshock) that may be mediated by the extraordinary contractility of rhizoplasts (50), with normal coordination after abrupt gait changes rapidly reestablished. Fibrillar structures under tension experience much distortion during *active* beating, as observed from misalignment of fiber striation patterns (70). Contraction during live beating is ATP-dependent in *Polytomella* (71), occurs in real-time in paralyzed flagella and temperature sensitive mutants of *Chlamydomonas* (72), and to an extraordinary degree in *Microthamnion* zoospores (73). ATPase activity has also been identified in the rod cells of the human eye where a large striated root attaches to the BB of a short (non-motile) cilium (74). Attachment sites of contractile fibers also exhibit great specificity, in most species to specific microtubule triplets and disc complexes. In *P. octopus* contractile fibers attach to the "weaker" side of BBs (triplets 6-9), and may function to pull the flagellum back from each power stroke during its unique multi-breaststroke gait.

Evolution of multiflagellation among Viridiplantae. As an appendage, cilia, flagella and its $9+2$ axoneme prevails across eukaryotes and especially the green algae; yet beyond the universality of this basic machinery much variability (Fig. 5) persists in the placement of organelles, form of flagellar insertion, and diversity of flagellar coordination. The basal apparatus is that rare structure which is both universally distributed and stable enough to infer homology across large phylogenetic distances, and yet variable enough to distinguish between different lineages. Representative species considered here express 2^n flagella, with much conservatism in the bi- or quadri- flagellate condition. Since an early flagellate phagocytosed a prokaryote (the future chloroplast) $>$1 billion years ago, green algae have evolved photosynthesis and autotrophism (75). Their radiation and division into the Streptophyta and Chlorophyta (27) has been corroborated by modern high-throughput chloroplast genome sequencing (77). Occupying a basal phylogenetic position are morphologically diverse species of freshwater and marine *Prasinophytes*, including the *Pyramimonas* species (20) studied here. These have conspicuous body and flagella scales which are precursors of theca and *Volvocalean* cell walls (53). In particular *P. tetrarhynchus*, *P. octopus*, and *P. cyrtoptera* are assigned according to morphological characters (78) to the same subgenus, in which accelerated rates of evolution were confirmed by cladistic analysis of *rbcL* gene sequences (Fig. 5). Changes in basal ultrastructure were major events (20) with the quadriflagellate condition arising multiple times, in fact it is the quadriflagellates (e.g. *Carteria*) and not Chlamydomonad-type biflagellates that are considered basal to advanced Volvocales (77, 79). The advanced heterotrophic alga *Polytomella*, thought to have evolved by cell doubling along a direct line of descent from CR (80), displays the same trot gait as the ancestral *P. parkeae*. In these cases, convergent ultrastructural modifications coincident with multiplicity and doubling of BBs may have evolved to enable strong coupling between opposite flagella pairs.

The sparsity of species bearing >4 localized flagella (*P. octopus*, *P. cyrtoptera*) may stem from the difficulty and activity costs of a flagellar apparatus capable of maintaining coordination from within despite external effects such as hydrodynamics. *P. cyrtoptera* exemplifies an intermediate between few to many flagella (16 is the highest number ever reported in a phytoflagellate (44)), and able to exploit hydrodynamics for swimming in a novel manner (Fig. 5). The energetic gains of such cooperativity may have inspired derivation of multiflagellated colonial volvocales from unicellular ancestors. Opportunities for fluid-mediated flagellar coordination and metachronism imposes new constraints on the configuration of flagella and BBs. In VC somatic cells for example, BBs reorient during early stages of development to become parallel (Fig. 1C), while biflagellate VC sperm cells (required to swim independently) retain the primitive V-formation.

Implications for active control of flagellar coordination. From the comparative studies carried out in this work we conclude that the physical principle for coordinating collective ciliary beating in *Volvox* or *Paramecium* differs from that responsible for defining precise patterns of beating in unicellular microswimmers bearing only few flagella. In the former case hydrodynamic coupling between flagella is sufficient (12), but in the latter (especially for obligate autotrophs) there is far greater incentive for efficient swimming to be robust *in spite of* hydrodynamic perturbations. Even in arrays of mammalian cilia, ciliary roots and basal feet structures continue to provide additional resistance to fluid stresses (22, 81).

Rapid changes in cellular structure that are of fundamental evolutionary interest may have arisen in the first instance in green flagellates than higher organisms. At the base of flagella in these algae are found diverse networks of interconnecting filaments that are not only responsible for anchorage and placement of flagella but which must now also be implicated in defining the symmetries of flagellar coordination. In CR for instance, most basal body connections do not appear until *after* the BBs have already formed. Fiber contractility can produce elastic coupling between BBs to force nearby flagella into modes of synchrony (IP or AP) that oppose hydrodynamic influences (15, 82). This elasticity may be actively modulated, highlighting a direct correlation between cellular physiology and flagellar beating that has already been identified (27, 83). Further insights into such processes will certainly require additional modelling and experimentation. The rapidity with which patterns of synchrony can change is suggestive of transduction by electrical signals or ionic currents (84), which may be effected from cell interior to flagella by changes in the

state of contraction or relaxation of connecting fibers. Striations of algal rhizoplasts are even biochemically mutable in a manner reminiscent of mammalian muscle. We are therefore led to suggest that a parallel evolution of neuromuscular control of appendages may have occurred much earlier than previously thought (50, 85).

Materials and Methods

Culturing and growth of algae. Below are brief descriptions of the protocols for species whose flagellar dynamics are studied here.

Volvox. V. carteri was prepared as described elsewhere (12). The remaining species, unless otherwise specified, were maintained under controlled illumination on $14:10$ day/night cycles, and at a constant temperature of 22°C (incubation chamber, Binder).

Pyramimonas. Marine species obtained from the Scandanavian Culture Collection of Algae and Protozoa, K-0006 *P. parkeae* R.E. Norris et B.R. Pearson 1975 (subgenus *Trichocystis*), K-0001 *P. octopus* Moestrup et Aa. Kristiansen 1987 (subgenus *Pyramimonas*), and K-0382 *P. cyrtoptera* Daugbjerg 1992 (subgenus *Pyramimonas*), were cultured in TL30 medium (86). Of these, *P. cyrtoptera* is an Arctic species and was cultured at 4°C. A fourth *Pyramimonas*, K-0002 *P. tetrarhynchus* Schmarda 1850 (type species) is a freshwater species, and was grown in an enriched soil medium NF2 (86).

Tetraselmis. Marine species *T. suecica* (gift from University of Cambridge Department of Plant Sciences) and *T. subcordiformis* (CCAP 116/1A), were cultured in the f/2 medium (87).

Polytoma. P. uvella Ehrenberg 1832 (CCAP 62/2A) was grown in polytoma medium (comprising 2% sodium acetate trihydrate, 1% yeast extract and 1% bacterial tryptone (87)).

Polytomella. Two species (CCAP 63/1 and CCAP 63/3) were maintained on a biphasic soil/water medium (87).

Carteria. C. crucifera Korschikov ex Pascher (1927) from CCAP (8/7C) was grown in a modified Bold basal medium (87).

Chlamydomonas. C. reinhardtii strains were obtained from the Chlamydomonas Collection, wildtype CC125, and variable flagella mutant *vfl3* (CC1686), and grown photoautotrophically in liquid culture (Tris-Acetate Phosphate).

Production of quadriflagellate dikaryons. High-mating efficiency strains of *C. reinhardtii* CC620 (mt^{+}), CC621 (mt^{-}) were obtained from the Chlamydomonas Collection, and grown photoautotrophically in nitrogen-free TAP to induce formation of motile gametic cells of both mating types. Fusing of gametes occurred under constant white light illumination.

Manipulation of viscosity. To facilitate identification of flagella in certain species, the viscosity of the medium was increased by addition of Methyl cellulose (M7027, Sigma Aldrich, 15 cP) to slow down cell rotation and translation rates.

Microscopy and micromanipulation. The capture of single cells are as described elsewhere (12, 14, 16, 27). For Fig. 3A caught CR cells were examined under the light microscope to identify the eyespot and thus *cis* and *trans* flagella; the correct flagellum was then carefully removed using a second pipette with smaller inner diameter.

ACKNOWLEDGMENTS. This work is supported by a Junior Research Fellowship from Magdalene College Cambridge (KYW) and a Wellcome Trust Senior Investigator Award (REG). We thank Kyriacos Leptos and Marco Polin for discussions relating to the contractility of the basal apparatus at an early stage of this work, and the possible insights provided by the vfl class of mutants, François Peaudecerf for kindly providing the CR gametes, Matthew Herron, Thomas Pröschold and Stephanie Höhn for valuable comments on the manuscript.

References

1. Machemer H (1972) Ciliary activity and origin of metachromy in *Paramecium* - effects of increased viscosity. *J. Exp. Biol*. 57(1):239–259.
2. Goldstein RE (2015) Green algae as model organisms for biological fluid dynamics. *Annu. Rev. Fluid Mech*. 47:343–375.
3. Orme BAA, Otto SR, Blake JR (2001) Enhanced efficiency of feeding and mixing due to chaotic flow patterns around choanoflagellates. *IMA J. Math. Appl. Medicine Biol*. 18(3):293–325.
4. Kramer-Zucker AG et al. (2005) Cilia-driven fluid flow in the zebrafish pronephros, brain and kupffer's vesicle is required for normal organogenesis. *Development*. 132(8):1907–1921.
5. Guirao B, Joanny JF (2007) Spontaneous creation of macroscopic flow and metachronal waves in an array of cilia. *Biophys. J*. 92(6):1900–1917.
6. Lechtreck KF, Sanderson MJ, Witman GB (2009) High-speed digital imaging of ependymal cilia in the murine brain. *Cilia: Struct. Motil*. 91:255–264.
7. Smith DJ, Gaffney EA, Blake JR (2008) Modelling mucociliary clearance. *Respir. Physiol. & Neurobiol*. 163(1-3):178–188.
8. Gray J (1928) *Ciliary Movement*. (Cambridge University Press).
9. Rothschild (1949) Measurement of sperm activity before artificial insemination. *Nature*. 163(4140):358–359.
10. Riedel IH, Kruse K, Howard J (2005) A self-organized vortex array of hydrodynamically entrained sperm cells. *Science*. 309(5732):300–303.
11. Gueron S, Levit-Gurevich K (1999) Energetic considerations of ciliary beating and the advantage of metachronal coordination. *Proc. Natl. Acad. Sci. United States Am*. 96(22):12240–12245.
12. Brumley DR, Wan KY, Polin M, Goldstein RE (2014) Flagellar synchronization through direct hydrodynamic interactions. *elife* 3:e02750.
13. Solari CA et al. (2011) Flagellar phenotypic plasticity in volvocalean algae correlates with Péclet number. *J. Royal Soc. Interface* 8(63):1409–1417.
14. Brumley DR, Polin M, Pedley TJ, Goldstein RE (2012) Hydrodynamic synchronization and metachronal waves on the surface of the colonial alga *Volvox carteri*. *Phys. Rev. Lett*. 109(26):268102.
15. Leptos KC et al. (2013) Antiphase synchronization in a flagellar-dominance mutant of *Chlamydomonas*. *Phys. Rev. Lett*. 111:158101.
16. Wan KY, Leptos KC, Goldstein RE (2014) Lag, lock, sync, slip: the many "phases" of weakly coupled flagella. *J. Royal Soc. Interface* 11:20131160.
17. Huygens C (1673) *Horologium Oscillatorium, sive, De motu pendulorum ad horologia aptato demostrationes geometricae*. (F. Muguet,).
18. Ringo DL (1967) Flagellar motion and fine structure of flagellar apparatus in *Chlamydomonas*. *J. Cell Biol*. 33(3):543–&.
19. Inouye I (1993) Flagella and flagellar apparatuses of algae. *Ultrastruct. microalgae* pp. 99–133.
20. Irvine D, John D, eds. (1984) *The Systematics Association special volume Systematics of the green algae*, Systematics Association. (Academic Press) Vol. 27.
21. Kunimoto K et al. (2012) Coordinated ciliary beating requires odf2-mediated polarization of basal bodies via basal feet. *Cell* 148(1-2):189–200.
22. Galati FD et al. (2014) Disap-dependent striated fiber elongation is required to organize ciliary arrays. *J. Cell Biol*. 207(6):705–715.
23. Mcfadden GI, Schulze D, Surek B, Salisbury JL, Melkonian M (1987) Basal body reorientation mediated by a Ca^{2+}-modulated contractile protein. *J. Cell Biol*. 105(2):903–912.
24. Carl C, de Nys R, Lawton RJ, Paul NA (2014) Methods for the induction reproduction in a species of filamentous ulva. *PLOS One* 9(5):e97396.
25. Gilbert FA (1927) On the occurrence of biflagellate swarm cells in certain myxomycetes. *Mycologia*. 19:277–283.
26. Dieckmann CL (2003) Eyespot placement and assembly in the green alga *Chlamydomonas*. *Bioessays* 25(4):410–416.
27. Wan KY, Goldstein RE (2014) Rhythmicity, recurrence, and recovery of flagellar beating. *Phys. Rev. Lett*. 113(23):238103.
28. Ruffer U, Nultsch W (1987) Comparison of the beating of *Cis*-flagella and *Trans*-flagella of *Chlamydomonas* cells held on micropipettes. *Cell Motil. Cytoskelet*. 7(1):87–93.
29. Goldstein RE, Polin M, Tuval I (2009) Noise and synchronization in pairs of beating eukaryotic flagella. *Phys. Rev. Lett*. 103(16):168103.
30. Bruot N, Kotar J, de Lillo F, Lagomarsino MC, Cicuta P (2012) Driving potential and noise level determine the synchronization state of hydrodynamically coupled oscillators. *Phys. Rev. Lett*. 109(16):164103.
31. Geyer VF, Jülicher F, Howard J, Friedrich BM (2013) Cell-body rocking is a dominant mechanism for flagellar synchronization in a swimming alga. *Proc. Natl. Acad. Sci. United States Am*. 110(45):18058–18063.
32. Quaranta G, Aubin-Tam M, Tam D (2015) On the role of hydrodynamics vs intracellular coupling in synchronization of eukaryotic flagella. *Phys.*

Rev. Lett. 115(23):238101.
33. Witman GB (1993) *Chlamydomonas* phototaxis. *Trends Cell Biol*. 3(11):403–408.
34. Lewin RA (1952) Studies on the flagella of algae .1. general observations on *Chlamydomonas moewusii* Gerloff. *Biol. Bull*. 103(1):74–79.
35. Hyams JS, Borisy GG (1978) Isolated flagellar apparatus of *Chlamydomonas* - characterization of forward swimming and alteration of waveform and reversal of motion by calcium-ions invitro. *J. Cell Science*. 33(OCT):235–253.
36. Wright RL, Choknacki B, Jarvik JW (1983) Abnormal basal-body number, location, and orientation in a striated fiber-defective mutant of *Chlamydomonas reinhardtii*. *J. Cell Biol*. 96(6):1697–1707.
37. Wright RL, Salisbury JL, Jarvik JW (1985) A nucleus-basal body connector in *Chlamydomonas reinhardtii* that may function in basal body localization or segregation. *J. Cell Biol*. 101(5):1903–1912.
38. Geimer S, Melkonian M (2004) The ultrastructure of the *Chlamydomonas reinhardtii* basal apparatus: identification of an early marker of radial asymmetry inherent in the basal body. *J. Cell Science*. 117(13):2663–2674.
39. Hoops HJ, Wright RL, Jarvik JW, Witman GB (1984) Flagellar waveform and rotational orientation in a *Chlamydomonas* mutant lacking normal striated fibers. *J. Cell Biol*. 98(3):818–824.
40. Niedermayer T, Eckhardt B, Lenz P (2008) Synchronization, phase locking, and metachronal wave formation in ciliary chains. *Chaos* 18(3):037128.
41. Elfring GJ, Lauga E (2009) Hydrodynamic phase locking of swimming microorganisms. *Phys. Rev. Lett*. 103(8):088101.
42. Stewart KD, Mattox KR (1978) Structural evolution in flagellated cells of green-algae and land plants. *Biosystems*. 10(1-2):145–152.
43. Melkonian M (1980) Ultrastructural aspects of basal body associated fibrous structures in green-algae - a critical-review. *Biosystems*. 12(1-2):85–104.
44. Daugbjerg N, Moestrup O (1992) Ultrastructure of *Pyramimonas cyrtoptera* sp-nov (Prasinophyceae), a species with 16 flagella from nortratesFoxe basin, arctic Canada, including observations on growth rates. *Can. J. Bot. Can. De Bot*. 70(6):1259–1273.
45. Conrad W (1939) Notes protistologique. xi. sur *Pyramidomonas amylifera* n. sp. *Bull. R. Hist. Nat. Belg*. 15:1–10.
46. Hargraves P, Gardiner W (1980) The life history of *Pyramimonas amylifera* Conrad (Prasinophyceae). *J. plankton research* 2(2):99–108.
47. Hori T, Moestrup O (1987) Ultrastructure of the flagellar apparatus in *Pyramimonas octopus* (Prasinophyceae).1. axoneme structure and numbering of peripheral doublets triplets. *Protoplasma* 138(2-3):137–148.
48. Sym SD, Piernaar RN (1991) Ultrastructure of *Pyramimonas norrisii* sp nov (Prasinophyceae). *Br. Phycol. J*. 26(1):51–66.
49. Manton I (1968) Observations on the microanatomy of the type species of *Pyramimonas* (*P. tetrarhynchus* Schmarda). *Proc. Linn. Soc. Lond* 179(2):147–152.
50. Salisbury JL, Floyd GL (1978) Calcium-induced contraction of rhizoplast of a quadriflagellate green-alga. *Science*. 202(4371):975–977.
51. Collins JJ, Stewart IN (1993) Coupled nonlinear oscillators and the symmetries of animal gaits. *J. Nonlinear Science*. 3(3):349–392.
52. Schoner G, Jiang WY, Kelso JAS (1990) A synergetic theory of quadrupedal gaits and gait transitions. *J. Theor. Biol*. 142(3):359–391.
53. O'Kelly CJ, Floyd GL (1983) Flagellar apparatus absolute orientations and the phylogeny of the green algae. *Biosystems*. 16(3-4):227–251.
54. Moestrup O, Hori T (1989) Ultrastructure of the flagellar apparatus in *Pyramimonas octopus* (Prasinophyceae) .2. flagellar roots, connecting fibers, and numbering of individual flagella in green-algae. *Protoplasma* 148(1):41–56.
55. Norris RE, Pearson BR (1975) Fine structure of *Pyramimonas parkeae* new species Chlorophyta Prasinophyceae. *Arch. fuer Protistenkunde* 117(1-2):192–213.
56. Brown DL, Massalski A, Paternaude R (1976) Organization of flagellar apparatus and associated cytoplasmic microtubules in quadriflagellate alga *Polytomella agilis*. *J. Cell Biol*. 69(1):106–125.
57. Salisbury JL, Swanson JA, Floyd GL, Hall R, Maihle NJ (1981) Ultrastructure of the flagellar apparatus of the green alga *Tetraselmis subcordiformis* - with special consideration given to the function of the rhizoplast and rhizanchora. *Protoplasma* 107(1-2):1–11.
58. Lembi CA (1975) Fine-structure of flagellar apparatus of *Carteria*. *J. Phycol*. 11(1):1–9.
59. Harris EH (2009) *The Chlamydomonas sourcebook. A comprehensive guide to biology and laboratory use.*
60. Hausman K, Radek R, eds. (2014) *Cilia and flagella, ciliates and Flagellates: ultrastructure and cell biology, function and systematics, symbiosis and biodiversity*. (Schweizerbart Science Publishers).
61. Beech PL, Heimann K, Melkonian M (1991) Development of the flagellar apparatus during the cell-cycle in unicellular algae. *Protoplasma* 164(1-3):23–37.
62. Sun D, Roth S, Black MJ (2014) A quantitative analysis of current practices in optical flow estimation and the principles behind them. *Int. J. Comput. Vis*. 106(2):115–137.
63. Daugbjerg N, Moestrup O, Archtander P (1994) Phylogeny of the genus *Pyramimonas* (Prasinophyceae, Chlorophyta) inferred from the rbcL gene. *J. Phycol*. 30(6):991–999.
64. Okita N, Isogai N, Hirono M, Kamiya R, Yoshimura K (2005) Phototactic activity in *Chlamydomonas* 'non-phototactic' mutants deficient in Ca^{2+}-dependent control of flagellar dominance or in inner-arm dynein. *J. Cell Science*. 118(3):529–537.
65. Kamiya R, Witman GB (1984) Submicromolar levels of calcium control the balance of beating between the two flagella in demembranated models of *Chlamydomonas*. *Cell Motil. Cytoskelet*. 98(1):97–107.
66. Bessen M, Fay RB, Witman GB (1980) Calcium control of waveform in isolated flagellar axonemes of *Chlamydomonas*. *J. Cell Biol*. 86(2):446–455.
67. Mukundan V, Sartori P, Geyer VF, Jülicher F, Howard J (2014) Motor regulation results in distal forces that bend partially disintegrated *Chlamydomonas* axonemes into circular arcs. *Biophys. J*. 106(11):2434–2442.
68. Melkonian M (1983) Functional and phylogenetic aspects of the basal apparatus in algal cells. *J. Submicrosc. Cytol. Pathol*. 15(1):121–125.
69. Salisbury JL (1988) The lost neuromotor apparatus of *Chlamydomonas* - rediscovered. *J. Protozool*. 35(4):574–577.
70. Gibbons IR, Grimstone AV (1960) On flagellar structure in certain flagellates. *J. Biophys. Biochem. Cytol*. 7(4):697–&.
71. White RB, Brown DL (1981) ATPase activities associated with the flagellar basal apparatus of *Polytomella*. *J. Ultrastruct. Res*. 75(2):151–161.
72. Hayashi M, Yagi T, Yoshimura K, Kamiya R (1998) Real-time observation of Ca^{2+}-induced basal body reorientation in *Chlamydomonas*. *Cell Motil. Cytoskelet*. 41(1):49–56.
73. Watson MW (1975) Flagellar apparatus, eyespot and behavior of *Microthamnion kuetzingianum* (Chlorophyceae) zoospores. *J. Phycol*. 11(4):439–448.
74. Matsusaka T (1967) ATPase activity in the ciliary rootlet of human retinal rods. *The J. cell biology* 33(1):203–8.
75. Cavalier-Smith T (1982) The origins of plastids. *Biol. J. Linnean Soc*. 17(3):289–306.
76. Leliaert F et al. (2012) Phylogeny and molecular evolution of the green algae. *Critical Rev. In Plant Sci*. 31(1):1–46.
77. Buchheim MA et al. (1996) Phylogeny of the Chlamydomonadales (Chlorophyceae): A comparison of ribosomal RNA gene sequences from the nucleus and the chloroplast. *Mol. Phylogenetics Evol*. 5(2):391–402.
78. Mcfadden GI, Hill D, Wetherbee R (1986) A study of the genus pyramimonas (prasinophyceae) from southeastern Australia. *Nord. J. Bot*. 6(2):209–234.
79. Nozaki H, Misumi O, Kuroiwa T (2003) Phylogeny of the quadriflagellate Volvocales (Chlorophyceae) based on chloroplast multigene sequences. *Mol. Phylogenetics Evol*. 29(1):58–66.
80. Smith DR, Lee RW (2014) A plastid without a genome: Evidence from the nonphotosynthetic green algal genus Polytomella. *Plant Physiol*. 164(4):1812–1819.
81. Brooks ER, Wallingford JB (2014) Multiciliated cells. *Curr. Biol*. 24(19):R973–R982.
82. Cosentino Lagomarsino M, Jona P, Bassetti B (2003) Metachronal waves for deterministic switching two-state oscillators with hydrodynamic interaction. *Phys. Rev. E* 68(2):021908.
83. Ma R, Klindt GS, Riedel-Kruse IH, Jülicher F, Friedrich BM (2014) Active phase and amplitude fluctuations of flagellar beating. *Phys. Rev. Lett*. 113(4):048101.
84. Harz H, Hegemann P (1991) Rhodopsin-regulated calcium currents in *Chlamydomonas*. *Nature*. 351(6326):489–491.
85. Jékely G, Paps J, Nielsen C (2015) The phylogenetic position of ctenophores and the origin(s) of nervous systems. *Evodevo* 6:1.
86. (2015) http://www.sccap.dk/media/.
87. (2015) http://www.ccap.ac.uk/pdfrecipes.htm.

SUPPLEMENTARY MATERIAL

We discuss here in more detail aspects of flagellar synchronization and swimming gaits in the unicellular green algae described in the text and SI Videos.

Pairwise synchrony: tri-flagellated CR mutant. The *vfl3* mutant lacking or defective in distal striated fibers characteristically exhibits a variable number of flagella, each with apparently normal intrinsic motility but aberrant orientation. As a result, the flagella belonging to the same cell display greater frequency variance than the wildtype. When frequencies are sufficiently close, nearby configurations of flagella appear to be subject to significant hydrodynamic interactions. In the cell shown (Fig. S1) this leads to a competition between IP and AP components.

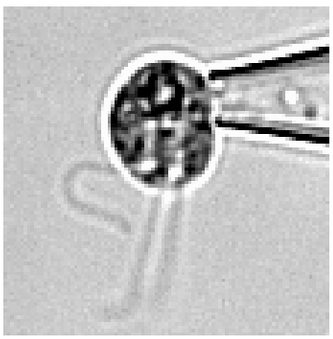

Fig. S1: Flagellar beating in the *vfl3* mutant. See also SI Video 1 and Fig. 2D. A cell with three flagella: the inner pair is oriented with power strokes in the same direction and tends towards IP synchrony, while the "outer" flagellum (leftmost) attempts to synchronize in antiphase with respect to the first pair.

Pairwise synchrony: two VC somatic cells. Here we elaborate on observed pairwise synchronization states between the flagella of two *V. carteri* somatic cells held in close proximity *and* with opposing power strokes, with particular emphasis on the consistency with theoretical predictions based on hydrodynamic interactions. As discussed in the main text, two states are observed (IP and AP), with the AP being preferred/more stable than the IP (Figs. 3 and S2). Transitions between IP and AP synchrony appear to be stochastic, stemming from inherent biochemical noise in the system. Within either state however, precise phase relationships are maintained. For interpolated flagellar phases $\phi_{1,2}$ ($\in [0, 2\pi]$) measured for each flagellum directly from the experimental data, we plot $\cos(\phi_{1,2})$ in SI Videos 2&3.

It is convenient and insightful to consider a dimension-reduced model in which each flagellum is modelled as a sphere of radius a constrained to oscillate along a near-circular trajectory of radius R (5). Let $\hat{\mathbf{e}}_{\phi_i} = (-\sin(\phi_i), \cos(\phi_i))$ and $\hat{\mathbf{e}}_{r_i} = (\cos(\phi_i), \sin(\phi_i))$ denote unit vectors in the tangential and radial directions for each flagellum n, and measure phases $\phi_{1,2}$ CCW from the +ve x-axis. The two spheres are centered at $\mathbf{r_{O}}_{1,2}$, separated by $\ell = |\mathbf{r_{O}}_2 - \mathbf{r_{O}}_1|$ which is assumed large so that $a \ll \ell$ and $R \ll \ell$ (i.e. hydrodynamic far field), but simulations and experimental studies on colloidal systems have shown that qualitative predictions of the theory are still applicable even in situations where these values are not so small.

The velocities are given by $\mathbf{u}_i = \dot{R}_i\hat{\mathbf{e}}_{r_i} + R_n\dot{\phi}_i\hat{\mathbf{e}}_{\phi_i}$. The orbital radius is assumed to be flexible, characterized by a spring constant k and natural length R_0. Even for a simple driving force (assumed proportional to angular velocity), this flexibility allows each sphere to respond to hydrodynamic perturbations arising from the motion of its neighbor thereby leading to trajectory deformations of the correct sign to achieve synchronization. More generally, we can incorporate an additional variable driving force so that, for example,

$$\mathbf{F}_i = -k(R_i - R_0)\hat{\mathbf{e}}_{R_i} + F(\phi_i)\hat{\mathbf{e}}_{\phi_i}, \qquad [1]$$

where

$$F(\phi_i) = F_0(1 - A\sin(2\phi_i)) \qquad [2]$$

acting tangentially along the orbit (2). The functional form of $F(\phi)$ has been chosen following Uchida & Golestanian (3) to provide the simplest modulated force for near-circular trajectories; terms of higher order become negligible. Depending on orbital rigidity one or the other of the two contributions will dominate (7). For rapid synchronization of flagella, it has been shown that orbital compliance dominates over force modulation (12). For counter-rotating spheres, if we take $F(\phi_1) = F_0(1 - A\sin(2\phi_1))$ then $F(\phi_2) = -F_0(1 + A\sin(2\phi_2)))$.

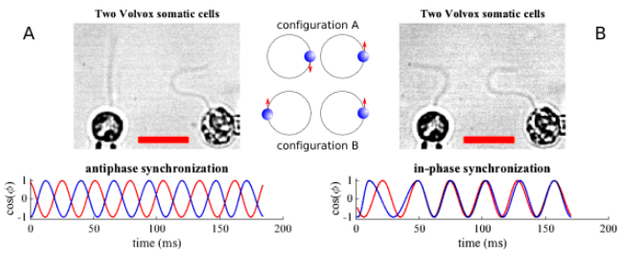

Fig. S2: Synchronization of flagella on *Volvox* somatic cells. As each flagellum is on a separate pipette-held cell, coupling is solely through the intervening fluid. The beating patterns correspond to configurations of counter-rotating spheres which tend to (A) AP or (B) IP states; state A is more stable and has a higher frequency than B, as predicted. See SI Videos 2&3. Scale bars are 10 μm.

Motion is described (1) by the force balance $\mathbf{u}_i = \mathbf{O}_{ij}\mathbf{F}_j$, where

$$\mathbf{O}_{ij} = \zeta^{-1}\left(\delta_{ij} + (1-\delta_{ij})\frac{3a}{4r_{ij}}\left(1 + \frac{\hat{\mathbf{r}}_{ij}\hat{\mathbf{r}}_{ij}}{r_{ij}^2}\right)\right), \quad (i,j = 1,2) \qquad [3]$$

where $\zeta = 6\pi\eta a$ is the drag coefficient of a sphere and $\hat{\mathbf{r}}_{ij} = (\mathbf{r}_j - \mathbf{r}_i)/r_{ij} \simeq \hat{\mathbf{x}} + \mathcal{O}(R/\ell)$. Force balance in the tangential and radial directions gives:

$$\begin{aligned}\zeta\dot{R}_i &= \epsilon\left(1 + \hat{\mathbf{x}}\hat{\mathbf{x}}\right)\mathbf{F}_i \cdot \hat{\mathbf{e}}_{R_i} - k(R_i - R_0) \qquad [4]\\ \zeta R_i\dot{\phi}_i &= F(\phi_i) + \epsilon\left(1 + \hat{\mathbf{x}}\hat{\mathbf{x}}\right)\mathbf{F}_i \cdot \hat{\mathbf{e}}_{\phi_i},\end{aligned}$$

where $\epsilon = 3a/4\ell$. If radial variations decay much faster than tangential ones, so $\dot{R} \simeq 0$, then $k(R_i - R_0) \sim \mathcal{O}(\epsilon)$, and we can further expand $\mathbf{F}_i/\zeta \approx R_i\dot{\phi}_i\hat{\mathbf{e}}_{\phi_i} + \mathcal{O}(\epsilon)$. The dynamics of oscillator 1 is then given by

$$\begin{aligned}\zeta\dot{\phi}_1 =& F_1(\phi_1) + \frac{\epsilon F_i(\phi_i)}{2R_0}[3\cos(\phi_1 - \phi_2) - \cos(\phi_1 + \phi_2)]\\ &- \frac{\epsilon F_i(\phi_i)F_j(\phi_j)}{2kR_0^2}[3\sin(\phi_1 - \phi_2) - \sin(\phi_1 + \phi_2)], \qquad [5]\end{aligned}$$

and similarly for oscillator 2 under interchange of $1 \leftrightarrow 2$.

For counter-rotating spheres the phase sum $\Xi = \phi_1 + \phi_2$ fluctuates about $\Xi_0 = 0$ or $\Xi_0 = \pi$ in either AP or IP states. In the case of AP synchrony, let $\Xi = \Xi_0 + \delta$, then $\phi_2 = \phi$, and $\phi_1 = \delta - \phi$, and we have

$$\begin{aligned}\zeta\frac{\dot{\delta}}{\delta} \simeq& -2\frac{F_0 A}{R_0}\cos(\phi) - \frac{\epsilon F_0 A}{R_0}\cos(2\phi)(3\cos(2\phi) - 1)\\ &- \frac{\epsilon F_0^2}{kR_0^2}(1 + A\sin(2\phi))^2,\end{aligned}$$

and similarly for the IP state - for a change of sign to the last term in the above. This last term corresponds to elastic deformation of orbits, and is < 0 (leading to stability) for all phases ϕ in the case of AP synchronization but > 0 (leading to instability) in the case of IP synchronization, consistent with our experimental observations. Furthermore the average period $T_{\text{AP, IP}}$ of these metastable states is then given by $\int_0^{2\pi}\dot{\phi}^{-1}\,d\phi$ (4):

$$T_{\text{AP, IP}} = \frac{2\pi\zeta R_0}{F_0\sqrt{1 - A^2}}\left(1 \mp \frac{1}{2}\epsilon\right). \qquad [6]$$

From the data, we find the experimental configuration to be consistent with $a \simeq 3$ μm for a separation of $\ell \simeq 15$ μm; in particular, the AP state is indeed faster than the IP.

Mechanical perturbation of flagellar beating The marine quadriflagellate *T. suecica* swims with a characteristic transverse gallop (Fig. 4) when free or pipette-held. The presence of theca renders them amenable to micromanipulation. SI Video 5 compares a pipette-held cell with flagella that are free to beat, with the same cell some time later after beating is stalled in one of its four flagella by careful application of suction (which traps the flagellum inside the pipette). The prior coordination in the remaining flagella is retained despite the significant change in hydrodynamic loading.

Systematics and ultrastructure of the green algae. The species of green algae referenced in this study are presented in full in Fig. 5. Here, we provide some additional details and references for the interested reader.

According to the most current classification, the Viridiplantae comprises two phyla: the Streptophyta – which contains many freshwater Charophyta algae and most land plants, and the Chlorophyta – which is the relevant category for most green algae. The precise evolutionary history of the Chlorophyta has proved rather difficult to elucidate, in the current consensus there are three core classes (Chlorophyceae: C, Trebouxiophyceae: T, and the Ulvophyceae: U), and a fourth non-monophyletic class of more primitive algae known collectively as the "Prasinophyceae".

Earlly attempts to classify the green algae by morphological form (unicellular, colonial, filamentous) (9) were superseded by schemes based on comparisons of basal body (BB) ultrastructure (microtubular roots, orientation of basal bodies etc) (11, 12, 20). The Prasinophyte algae have counter-clockwise offset of basal bodies (now considered a primative trait), while in contrast the Chlorophyte algae are characterized by a clockwise offset (see for instance *Chlamydomonas*, Fig. 1D). Later molecular approaches soon became available, involving the use of genetic markers based on ribosomal (SSU rDNA) or chloroplast genes such as *rbc*L, and used to verify or refine existing classifications. These were particularly important for distinguishing between species that were otherwise morphologically identical (20). Phylogenetic trees are then constructed based on these results via statistical methods such as maximum likelihood or maximum parsimony. The branching order and relative edge lengths shown on Fig. 5 were estimated from a composite of available maximum likelihood trees (14–21).

Most of the Prasinophyte algae considered in this study belong to the order Pyrmimonadales which reside at the base of the Chlorophyta and are considered to be the earliest green algae (11). These phytoflagellates have 4 to 16 flagella and are united by their lack of advanced Chlorophycean characters as well as by the presence of primitive scaly body coverings. The *Pyramimonas* genus, first described from a freshwater locality in Cambridge, England, has been shown to exhibit great morphological variability not just in the numbers of flagella but also the composition of types of organic scales (crown, square, box etc). According to *rbcL* sequencing, *Pyramimonas* does not constitute a monophyletic clade. At least four subgenera exists, namely *Pyramimonas*, *Vestigifera*, *Punctuate*, and *Trichocystis*, of these all four Pyramimonas species studied here (*P. parkeae*, *P. tetrarhynchus*, *P. octopus*, and *P. cyrtoptera*) belong to the same subgenus *Pyramimonas* (23). Chloroplast sequencing has also revealed accelerated rates of evolution in this monophyletic subgenus. The branching order among these four species is presented in Fig. 5, following Daugbjerg *et al* (16), and Harðardéttir *et al* (24). Only *P. tetrarhynchus* (the type species) is a freshwater species, the other three being marine. The prototypical *Pyramimonas* has four homodynamic and isokont flagella which emerge from an anterior pit, where the two oldest BBs are connected by a large synistosome which is striated in cross-section and thought to be contractile. Flagella beat away from each other in a roughly cruciate pattern, with some differences across species in the precise geometry of the four BBs, which form a diamond shape in most cases.

The final Prasinophycean alga in our list is *Tetraselmis* (12) (synonymous with *Platymonas*). It is considered very basal to the UTC clade, has a counterclockwise orientation of BBs, and is associated with early evolution of the plant phycoplast which is essential for the later emergence of multicellularity within the Chlorophyta. Along with *Scherffelia*, *Tetraselmis* is classified under the order Chlorodendrales (25, 26), which comprises thecate scaly flagellates, and were among the first green flagellates to evolve a rigid wall (theca). The presence of this bounding wall is thought to have prevented cell division in the flagellate state, contrary to *Pyramimonas*, which divides while remaining fully motile. In electron micrographs, the nucleus appears to be positioned centrally between the flagellar apparatus and pyrenoid.

The Chlamydomonadalean algae form the largest Chlorophyceae group and is taxonomically complex and diverse (14, 15); of the species studied here the genus *Carteria* is the most basal according to molecular phylogenetics, supporting the notion that the common ancestor of the core Chlorophyte algae may have been a Carteria-like quadriflagellate (21, 27). The biflagellate condition of *Chlamydomonas* may have resulted from a subsequent reduction from four flagella to two. Biflagellate Chlamydomonadales possess a CW rotation of the flagellar apparatus, and comprises mainly freshwater and terrestrial species. The favoured species *Chlamydomonas reinhardtii* and its multicellular relative *Volvox carteri* have been extensively studied as model organisms exemplifying the evolution to multcellularity (see also (27) and the many references therein). While many of these species are photoautotrophic, harnessing sunlight for energy through photosynthesis, a number have evolved into obligate heterotrophs. These include the colourless and wall-less algae *Polytoma* and *Polytomella* (13), which through the loss of chloroplasts have rather unusual mitochondrial or plastid genomes (22).

In Fig. 5, the illustrations of the basal apparatus represent simplified planar views only, please refer to the following external references for the detailed ultrastructure of each species featured in this work. In particular unlike the BBs of *Pyramimonas* which emerge almost parallel from a grove inside the cell, the BBs of Chlorophycean algae are often tilted with respect to each other, for instance the two BBs of *C. reinhardtii* are oriented at $70 - 100°$ (39) and those of *P. uvella* at $140°$ (42). BBs have also been numbered throughout according to the convention of Moestrup (35) by order of ontogenetic age wherever such information was available. i) *Pyramimonas parkeae* (29, 30), ii) *Pyramimonas tetrarhynchus* (31, 32), iii) *Pyramimonas octopus* (33–35), iv) *Pyramimonas cyrtoptera* (36), v) *Tetraselmis suecica* and *T. subcordiformis* (37, 38) vi) *Carteria crucifera* (28) (the basal apparatus of *Carteria* Group 2 is most peculiar, in which sigmoid shaped electron dense rods extend between opposite BB pairs) vii) *Chlamydomonas reinhardtii* (39), dikaryon (46) viii) *Volvox carteri* (40) ix) *Polytoma uvella* (43) (and for *Polytoma papillatum* (42)) x) *Polytomella parva* (synonymous with *P. agilis*) (41) .

Swimming with four flagella. Select species of quadriflagellates exemplify the possible gait symmetries. The motion is highly species-specific, where the patterns or sequence of actuation of the flagella appear to be independent of whether or not the cell body has been fixed in place.

Flagellar synchronization in a dikaryon of *Chlamydomonas*. Although CR is most likely to occur in its vegetative state, gametic cells capable of sexual reproduction can form under nitrogen deprivation in the presence of light. When two biflagellate CR gametes of opposite mating types ($+$ and $-$) come together, flagellar agglutination (44) occurs whereby the flagella of opposite mating types adhere strongly to each other (Figure. S3A1). This is followed by autolysin secretion which digests away the cell walls, after which a fertilization tubule extends from the $+$ gamete to its partner (Figure. S3A2). If fusion is successful, a single temporary dikaryon is formed, which is quadriflagellate (Figure. S3A3).

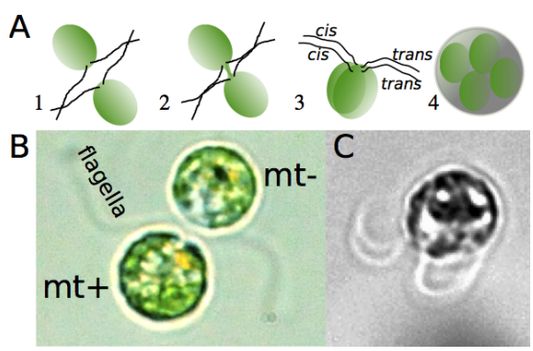

Fig. S3: Generation of a dikaryon of *Chlamydomonas*. For brevity, eyespot locations are not shown. (A) 1-4: Life cycle of sexual reproduction in CR. (B) A pair mating (stage 1). (C) A quadriflagellate dikaryon is formed. See SI Video 5.

These dikaryons exhibit a striking double bilateral breaststroke (in contrast to the double cruciate breaststroke observed in *P. parkeae*), in which pairs of flagella on the same side become strongly phase-synchronized. It is known that the flagella separate distally into *cis-cis* and *trans-trans* pairs, allowing cells to remain strongly phototactic during this period, which is another indication of good flagellar coordination. No new synthesis of basal body fibers occur, and indeed all traces of basal bodies and associated rootlets and fibers

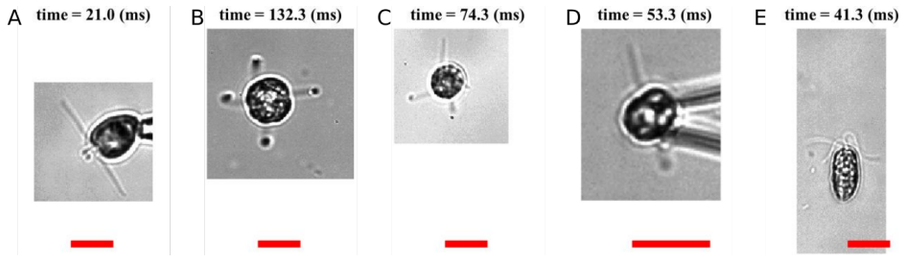

Fig. S4: Distinctive quadriflagellate gaits. See Fig. 6 of text and SI Video 6. (A) trot (*Pyramimonas parkeae*) held stationary by a micropipette, (B) pronk (*Pyramimonas tetrarhynchus*), (C) rotary gallop of *Carteria cruicifera* and of *Tetraselmis suecica* viewed apically when (D) held by micropipette or (E) freely-swimming. Scale bars are 10 μm.

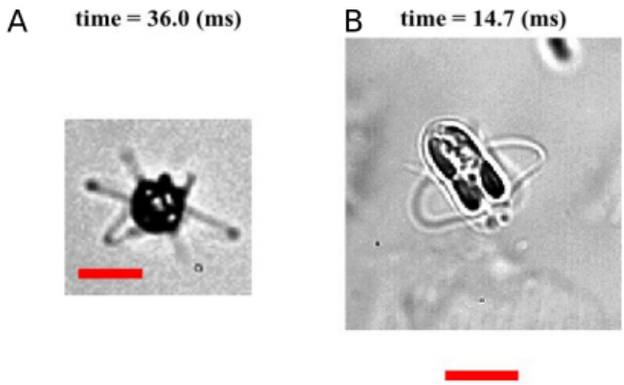

Fig. S5: Swimming dynamics of the octoflagellate *P. octopus*. (A) View from the top, where the cell is observed to rotate CCW about its long axis over time, and (B) view from the side, where several pairs of in-phase breaststrokes are observed, principally between diametrically opposed flagella. See SI Video 7. Scale bars are 10 μm.

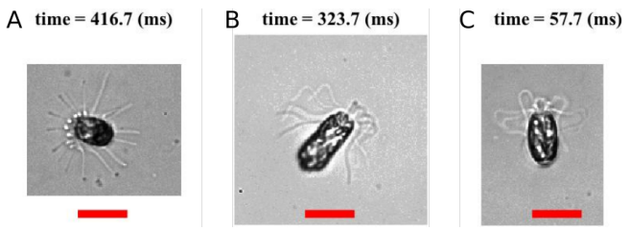

Fig. S6: Distinctive hexadecaflagellate gaits. (A) Pronk: all flagella synchronized (a hydrodynamic mode). (B) bilateral: one group comprising half of the flagella are synchronized, but are in anti-phase relative to the complementary group. (C) mixed mode: resembles a *P. octopus*. See SI Video 8. Scale bars are 20 μm.

dissolve within 6 hours after mating (45). Therefore there is a strong asymmetry in internal connectivity immediately upon formation of the quadriflagellate zygote, prior to the dissolution of the distal fibers between the original BBs (of like mating type), but lack of physical connections between pairs of BBs of unlike mating type (recall Fig. 5). Eventually, maturation of the zygotes leads to resorption of all flagella, and formation of a CR spore. These diploid zygotes await favorable conditions before release of 4 new haploid progeny, whereupon BBs are reassembled *de novo*.

Swimming with eight flagella. The octoflagellate *P. octopus* displays stochastic switching between a number of different gaits (Fig. S5 and SI Video 7). Primary among these is a complex breaststroke which appears to involve a number of phase-shifted pairwise IP breaststrokes. The IP synchrony within certain of the pairs are more robust than in others (the basal architecture is far from radially symmetric, with the large synistosome connecting BB1 and 2 (see Fig. 5).

Swimming with sixteen flagella. Flagellar coordination in the hexadecaflagelalte *P. cyrtoptera* leads to a number of distinctive gaits which may be dependent on the current state of contractile of the fiber network: three of which are shown here (Fig. S6 and SI Video 7. (A) Significant nearest-neighbour hydrodynamic effects can synchronize all sixteen flagella, which pronks with a well defined periodicity coinciding with the beat frequency of an individual flagellum. (B) The underlying basal-body network exhibits significant bilateral symmetry (Fig. 5), which could explain the frequent appearance of a bilateral gait in which flagella are divisible into two groups, which beat alternately. Flagella within each group appear to be strongly coupled in IP by hydrodynamic interactions. As a result the cell body sways periodically from side to side. C) In certain individuals, basal coupling appears strong enough to permit several phase-shifted breaststroke pairs and swimming is reminiscent of an octoflagellate with flagella doubled up in pairs - with the flagella in each pair undulating in perfect unison.

Emergence of metachronism in a hexadecaflagellate In *P. cyrtoptera*, neighboring flagella experience strong hydrodynamic interactions due to their close spatial proximity, giving rise to the striking pronking gait (SI Video 8) in which all sixteen flagella beat with zero relative phase difference. In this organism yet another phenomenon can be attributed to hydrodynamic synchronization: occasionally, we observe metachronal waves propagating circumferentially around the crown of flagella which become especially notable in cells swimming close to surfaces. We discuss below how this is consistent with theory concerning fluid-structure interactions near no-slip surfaces, and where dynamics are dominated by orbital compliance (Fig. S7).

Firstly, steric interactions near the wall forces the flagella to 'flatten' or reorient more laterally, contrary to the normal state in which they are recurved longitudinally along the cell body from the anterior to the posterior. This new orientation becomes more conducive to hydrodynamic coupling (see reference (14) of main text) between the flagella (Fig. S7A). Interactions are maximised when flagella are placed side-by-side and minimized when placed in the up/downstream directions. Secondly, proximity near the no-slip boundary itself means that the nearest-neighbor contribution to the coupling is increased, again encouraging the emergence of metachronal waves.

For the cell shown, a symplectic metachronal wave propagates CCW among its flagella, which causes the cell to rotate very slowly in a CW sense. We take the optical flow field $\mathbf{U}(\mathbf{r};t)$ as proxy for the real flow field in the vicinity of the organism (there is good agreement in direction even if flow magnitudes are less reliable). The time averaged flow field (Fig. S7) is clearly rotary

$$\langle \mathbf{U}(\mathbf{r};t)\rangle = \frac{1}{t}\int_0^t \mathbf{U}(\mathbf{r};t)\,dt$$

We decompose the flow into its radial and tangential components

$$\mathbf{U}(\mathbf{r};t) = U_r(\mathbf{r};t)\mathbf{e}_r + U_\theta(\mathbf{r};t)\mathbf{e}_\theta \qquad [7]$$

and concentrate on the radial component which corresponds the direction perpendicular to the wall, since forces perpendicular to a wall decay much faster than the tangential contribution. The plots reproduce features distinctive of a metachronal wave.

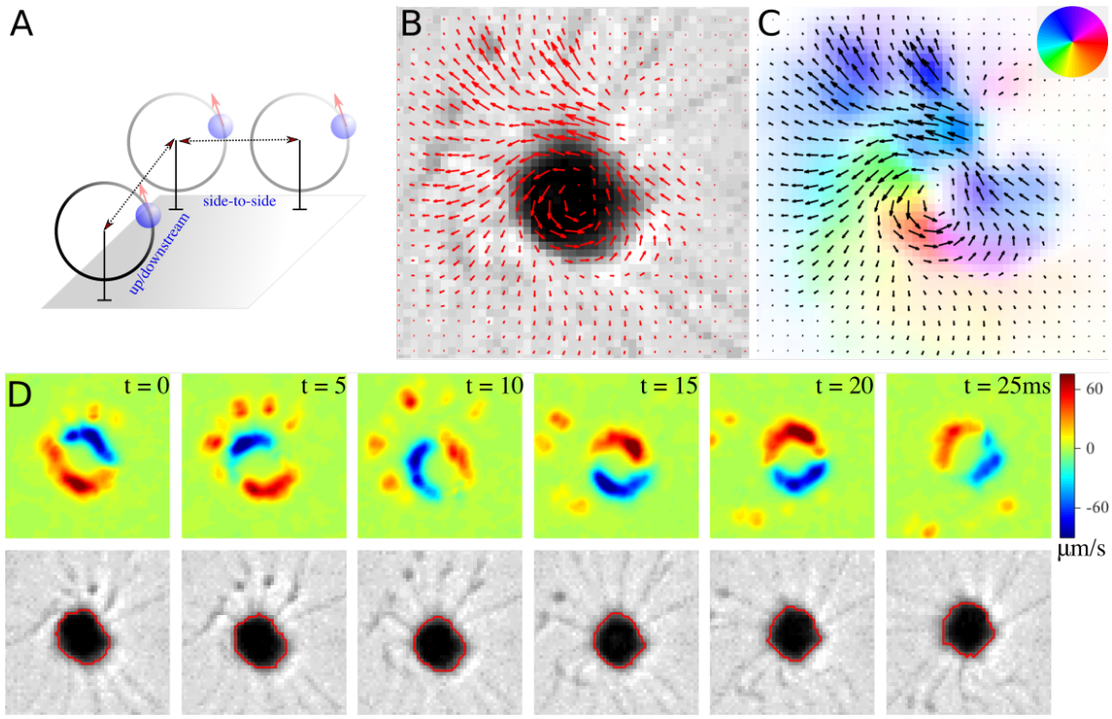

Fig. S7: Metachronism in a hexadecaflagellate. (A) The strength of hydrodynamic interactions between pairs of flagella is strongly dependent on their relative orientation. This leads to the formation of symplectic metachronal waves in a finite ring of flagellar oscillators, representing the hexadecaflagellate. (B,C) The average (optical) flow field $\langle \bar{U} \rangle$ around *P. crytoptera*. (D) Snapshots of the radial components of optical flow field.

Additional References

1. Happel J, Brenner H (1983) Low Reynolds number hydrodynamics: with special applications to particulate media. *Kluwer, New York*
2. Uchida G, Golestanian (2012) Hydrodynamic synchronization between objects with cyclic rigid trajectories. *The European Physical Journal E* 35: 1-14
3. Uchida N, Golestanian R (2011) Generic Conditions for Hydrodynamic Synchronization. *Phys. Rev. Lett* 106 (058104)
4. Box S, Debono L, Philips DB, Simpson SH (2015) Transitional behavior in hydrodynamically coupled oscillators. *Phys. Rev. E* 91 (022916)
5. Niedermayer T, Eckhardt B, Lenz P (2008) Synchronization, phase locking and metachronal wave formation in ciliary chains. *Chaos* 18 (037128)
6. Bruot N, Kotar J, de Lillo F, Cosentino Lagomarsino M, Cicuta P (2012) Driving potential and noise level determine the synchronization state of hydrodynamically coupled oscillators *Phys. Rev. Lett* 109 (164103)
7. Kotar J, Debono L, Bruot N, Box S, Philips DB, Simpson SH, Hanna S, Cicuta P (2013) Optimal hydrodynamic synchronization of colloidal oscillators. *Phys. Rev. Lett* 111 (228103)
8. Brumley DR, Polin M, Pedley TJ, Goldstein RE (2012) Hydrodynamic synchronization and metachronal waves on the surface of the colonial alga *Volvox carteri*. *Phys. Rev. Lett* 109 (268102)
9. Blackman F (1900) The primitive algae and the Flagellata. *Annals of Botany* 14: p647-688.
10. Irvine D, John D (1984) Systematics of the green algae *Academic Press, Oxford, England*
11. O'Kelly CJ, Floyd GL (1984) Flagellar apparatus absolute orientations and the phylogeny of the green algae. *Biosystems*16: p227-251
12. Mattox K, Stewart K (1984) Classification of the green algae: a concept based on comparative cytology. *Systematics of the green algae. The Systematics Association Special Volume 27, Academic Press, London and Orlando* p29-72
13. Rumpf R, Vernon D, Schreiber D, William Birky Jr D (1996) Evolutionary consequences of the loss of photosynthesis in Chlamydomonadaceae: phylogenetic analysis of Rrn18 (18S rDNA) in 13 Polytoma strains (Chlorophyta) *J. Phycol* 32: 119-126
14. Nakada T, Misawa K, Nozaki H (2008) Molecular systematics of the Volvocales (Chlorophyceae, Chlorophyta) based on exhaustive 18S rRNA phylogenetic analyses *Mol. Phylogenet. Evol* 48: 281-291
15. Nozaki H, Misumi O, Kuroiwa T (2003) Phylogeny of the quadriflagellate Volvocales (Chlorophyceae) based on chloroplast multigene sequences *Mol. Phylogenet. Evol* 29: 58-66
16. Daugbjerg N, Moestrup Ø, Arctander P (1994) Phylogeny of the genus Pyramimonas (Prasinophyceae, Chlorophyta) inferred from the rbcL gene *J. Phycol* 30: 991-999
17. Leliaert F, Verbruggen H, Zechman FW (2001) Into the deep: New discoveries at the base of the green plant phylogeny *Bioessays* 33: p683-692
18. Demchenko E, Mikhailyuk T, Coleman AW, Proschold T (2012) Generic and species concepts in Microglena (previously the Chlamydomonas monadina group) revised using an integrative approach *Eur. J. Phycol.* 47(3): p264-290
19. Cocquyt E (2009) Phylogeny and evolution of green algae (Fylogenie en moleculaire evolutie van groenwieren) *PhD thesis, Universiteit Ghent*
20. Pröschold T, Leliaert F (2007) Unravelling the algae: the past, present, and future of algal systematics (Chapter 7, Systematics of the green algae: conflict of classic and modern approaches) *CRC Press*
21. Buchheim M, Lemieux C, Otis C, Gutell RR, Chapman RL, Turmel M (1996) Phylogeny of the Chlamydomonadales (Chlorophyceae): A Comparison of Ribosomal RNA Gene Sequences from the Nucleus and the Chloroplast *Mol. Phylogenet. Evol* 5(2): p391-402
22. Smith DR, Hua J, Lee RW (2010) Evolution of linear mitochondrial DNA in three known lineages of Polytomella *Curr. Genet* 56: p427-438
23. Hori T, Moestrup Ø, Hoffman LR (2007) Fine structural studies on an ultraplanktonic species of Pyramimonas, P. virginica (Prasinophyceae), with a discussion of subgenera within the genus Pyramimonas *Eur. J. Phycol* 30(3): p219-234
24. Harðardéttir S, Lundholm N, Moestrup Ø, Nielson TG (2014) Description of Pyramimonas diskoicola sp. nov. and the importance of the flagellate Pyramimonas (Prasinophyceae) in Greenland sea ice during the winter-spring transition *Polar Biol* 37: p1479-1494
25. Wustman B, Melkonian M, Becker B (2004) A study of cell wall and flagella formation during cell division in the scaly green flagellate alga, Scherffelia dubia (Chlorophyta) *J. Phycol* 40: p895-910
26. Arora M, Chandrasheker A, Leliaert F, Delany J, Mesbahi E (2013) *Tetraselmis indica* (Chlorodendrophyceae, Chlorophyta), a new species

isolated from salt pans in Goa, India *Eur. J. Phycol* 48(1): 61-78
27. Leliaert F et al. (2012) Phylogeny and molecular evolution of the green algae. *Critical Rev. In Plant Sci.* 31(1): p1-46.
28. Lembi CA (1975) Fine-structure of flagellar apparatus of Carteria. *J. Phycol.* 11(1): p1-9.
29. Norris RE, Pearson BR (1975) Fine structure of Pyramimonas parkeae new species Chlorophyta Prasinophyceae. *Arch. fuer Protistenkunde* 117(1-2):p192-213.
30. Pienaar RN, Aken ME (1985) Fine structure of Pyramimonas pseudoparkeae sp. nov. (Prasinophyte) from South Africa *J. Phycol* 21: p428-447
31. Manton I (1968) Observations on the microanatomy of the type species of Pyramimonas (P. tetrarhynchus Schmarda). *Proc. Linn. Soc. Lond* 179(2): p147-152.
32. Belcher JH (1969) Further observations on the type species of Pyramimonas (P.tetrarhynchus Schmarda) (Prasinophyceae):anexamination by light microscopy, together with notes on its taxonomy. *Bot. J. Linn. Soc.* 62: 241-253.
33. Moestrup Ø, Hori T, Kristiansen A (1987) Fine structure of Pyramimonas octopus sp. nov., an octoflagellated benthic species of Pyramimonas (Prasinophyceae), with some observations on its ecology *Nord. J. Bot* 7(3): p339-352
34. Hori T, Moestrup Ø (1987) Ultrastructure of the flagellar apparatus in Pyramimonas octopus (Prasinophyceae).1. axoneme structure and numbering of peripheral doublets triplets. *Protoplasma* 138(2-3): p137-148.
35. Moestrup Ø, Hori T (1989) Ultrastructure of the flagellar apparatus in Pyramimonas octopus (Prasinophyceae) .2. flagellar roots, connecting fibers, and numbering of individual flagella in green-algae. *Protoplasma* 148(1): p41-56.
36. Daugbjerg N, Moestrup Ø (1992) Ultrastructure of Pyramimonas cyrtoptera sp-nov (Prasinophyceae), a species with 16 flagella from nortrates Foxe basin, arctic Canada, including observations on growth rates. *Can. J. Bot.* 70(6): p1259-1273.
37. Manton I, Parke M (1965) Observations of the fine structure of two species of Platymonas with special referennce to flagellar scales and the mode of origin of the theca *J. Mar. Biol. Ass. UK* 45: p743-754
38. Salisbury JL, Swanson JA, Floyd GL, Hall R, Maihle NJ (1981) Ultrastructure of the flagellar apparatus of the green alga Tetraselmis subcordiformis - with special consideration given to the function of the rhizoplast and rhizanchora. *Protoplasma*107(1-2): p1-11.
39. Ringo DL(1967) Flagellar motion and fine structure of flagellar apparatus in Chlamydomonas. *J. Cell Biol.* 33(3):p543-.
40. Kirk D (1998) *Volvox*: molecular-genetic origins of multicellularity and cellular differentiation *Developmental and Cell Biology Series, Cambridge University Press*
41. Brown DL, Massalski A, Paternaude R (1976) Organization of flagellar apparatus and associated cytoplasmic microtubules in quadriflagellate alga Polytomella agilis. *J. Cell Biol.* 69(1): p106-125.
42. Gaffal KP (1977) The relationship between basal bodies and the motility of *Polytoma papillatum* flagella *Experientia* 33(10): p1372-1374
43. Lang NJ (1963) Electron-Microscopic Demonstration of Plastids in *Polytoma J. Euk. Microbiol* 10(3): p333-339
44. Harris EH (2009) The *Chlamydomonas* Sourcebook: Introduction to Chlamydomonas and its laboratory use, *Academic Press, Oxford, England*
45. Cavalier-Smith T (1974) Basal body and flagellar development during the vegetative cell cycle and the sexual cycle of *Chlamydomonas reinhardtii J. Cell. Sci* 16: p529-556
46. Holmes JA, Dutcher SK (1989) Cellular asymmetry in *Chlamydomonas reinhardtii*, *Journal of Cell Science* 94: 273-285